
CHAPTER 17

Fuel

Prepared by

Mukesh Tayal and Milan Gacesa – Independent Consultants

Learning Objectives

The principal learning objectives of this chapter are:

- To gain a general understanding of the major mechanisms affecting fuel behaviour under normal operating conditions;
- To understand the underlying sciences of the relatively more important phenomena involving fuel, including fission gas release, internal gas pressure, thermal stresses, element deformation, environmentally assisted cracking, lateral vibrations of fuel elements, and fatigue of the bundle assembly weld; and
- To be able to perform calculations in the above subject areas to enable predictions.

Summary

Nuclear fuel, like conventional fuel, is responsible for generating heat and transferring the heat to a cooling medium. Unlike conventional fuel, nuclear fuel presents the additional challenge of retaining all the by-products of the heat-generating reaction within its matrix. Conventional fuel releases almost all its combustion by-products into the environment. Experience has shown that at times the integrity of CANDU fuel can be challenged while performing these roles. Eighteen failure mechanisms have been identified, some of which cause fission by-products to be released out of the fuel matrix. Other chapters in this book deal with preventing fission by-products which escape from the fuel matrix from reaching the public. CANDU reactors can locate and discharge fuel assemblies that release fission by-products into the coolant at power to minimize the effect of fuel defects on plant operation and the public. Acceptance criteria are established against which a fuel design is assessed to verify its ability to fulfill the design requirements without failing. A combination of analyzes and tests is used to complete the verification assessments.

Table of Contents

1	Introduction	4
2	Overview	5
2.1	Operating Environment	5
2.2	Fuel Design	6
2.3	In-Reactor Challenges	8
3	Power and Burnup	13
4	Collapsible Sheaths	14
4.1	Diametric Collapse	15
4.2	Longitudinal Ridging	16
4.3	Collapse into the Axial Gap	17
5	Thermal Performance of Fuel	18
6	Fission Gas and Internal Pressure	19
6.1	Overview	19
6.2	Recoil	24
6.3	Knockout	24
6.4	Diffusion of Fission Gas to Grain Boundaries	25
6.5	Internal Gas Pressure	25
7	Stresses and Deformations	26
7.1	Thermal Stresses in Pellets	27
7.2	Changes in Element Diameter and Length	28
8	Environmentally Assisted Cracking	31
8.1	EAC Processes	33
8.2	Defect Threshold	35
8.3	Defect Probability	36
8.4	Mitigation	38
9	Vibration and Fatigue	39
9.1	Alternating Stresses	39
9.2	Fatigue of the Endplate and the Assembly Weld	45
10	Fuel Design Verification	46
10.1	Damage Mechanisms	51
10.2	Acceptance Criteria and Integration	54
11	Operating Constraints and Inputs to the Safe Operating Envelope	59
12	Removal of Fuel Bundles Containing Defects	60
12.1	Deterioration of Primary Defects in Fuel Elements	60
12.2	Defect Removal Systems	62
12.3	Confirmation of Defect Removal	63
13	Closure	64
14	Problems	65
15	References	68
16	Further Reading	70
17	Relationships with Other Chapters	71
18	Acknowledgements	72

List of Figures

Figure 1 37-element CANDU fuel bundle.....	4
Figure 2 Causes of defects in CANDU fuel (1967–1996).....	10
Figure 3 Illustrative power histories.....	14
Figure 4 Sheath collapse: forms and stages.....	15
Figure 5 Illustrative permanent strain at the tip of a longitudinal ridge	16
Figure 6 Collapse into axial gap.....	17
Figure 7 Illustrative heat transfer and pellet temperature in a fuel element.....	18
Figure 8 Terms for fission gas release	20
Figure 9 Steady-state release of ^{88}Kr from a single crystal of UO_2	20
Figure 10 Grain boundary bubbles and tunnels	21
Figure 11 Changes in sizes and shapes of UO_2 grains during irradiation.....	22
Figure 12 Equiaxial grain growth.....	22
Figure 13 Columnar grain growth	23
Figure 14 Variation of internal gas pressure during irradiation	24
Figure 15 Typical cracks in a high-power pellet	27
Figure 16 Thermal stresses in a pellet	28
Figure 17 Removal of as-fabricated pores during irradiation	29
Figure 18 Fuel rod before and after startup	30
Figure 19 Causes of hourglassing in pellets	31
Figure 20 Power ramp cracks originating at a circumferential ridge	32
Figure 21 Power ramp cracks near a sheath/endcap junction	33
Figure 22 Key terms for environmentally assisted cracking during power ramps.....	33
Figure 23 Mechanism for power ramp failures.....	34
Figure 24 Defect threshold due to power ramp in non-CANLUB fuel at 140 ± 20 MWh/kgU.....	36
Figure 25 Defect probability.....	37
Figure 26 Lateral vibration of a fuel element.....	40
Figure 27 Endplate as a beam on elastic foundations	41
Figure 28 Stiffening of a fuel element at operating power.....	43
Figure 29 Margins in criteria and analyzes	57
Figure 30 Secondary hydriding.....	62
Figure 31 Schematic diagram of a delayed neutron monitoring system in a CANDU-6 reactor ..	63

List of Tables

Table 1 Illustrative design data for C6 fuel.....	11
Table 2 Illustrative data for fuel assessments	12
Table 3 Illustrative list of tests on prototype fuel bundles.....	47
Table 4 Fuel design acceptance criteria for normal operating conditions.....	54
Table 5 Illustrative list of computer codes used at AECL for fuel analyzes	58

1 Introduction

The principal roles of fuel are to generate heat and to maintain a reasonable geometry so that the coolant can carry that heat away. In addition, because fuel is a significant source of radiological hazard, appropriate fuel integrity needs to be ensured at all times—including during fabrication, operation, postulated accidents, and storage.

The science of the first two of these aspects, the generation and removal of heat, has been discussed in earlier chapters. In the current chapter, we focus on the science of those aspects of fuel that enable its reasonable integrity during normal operating conditions. Fuel integrity during accidents and during abnormal occurrences is covered in another chapter.

This chapter uses CANDU-6 (also called C6) fuel for illustration, as shown in Figure 1. The figure shows a fuel bundle in which fissile uranium is contained in 37 sealed fuel elements which are held together by two welded endplates. Separation of the hot fuel elements from each other, and from the pressure tube, is maintained by pads that are brazed to the fuel sheaths [Page, 1976].

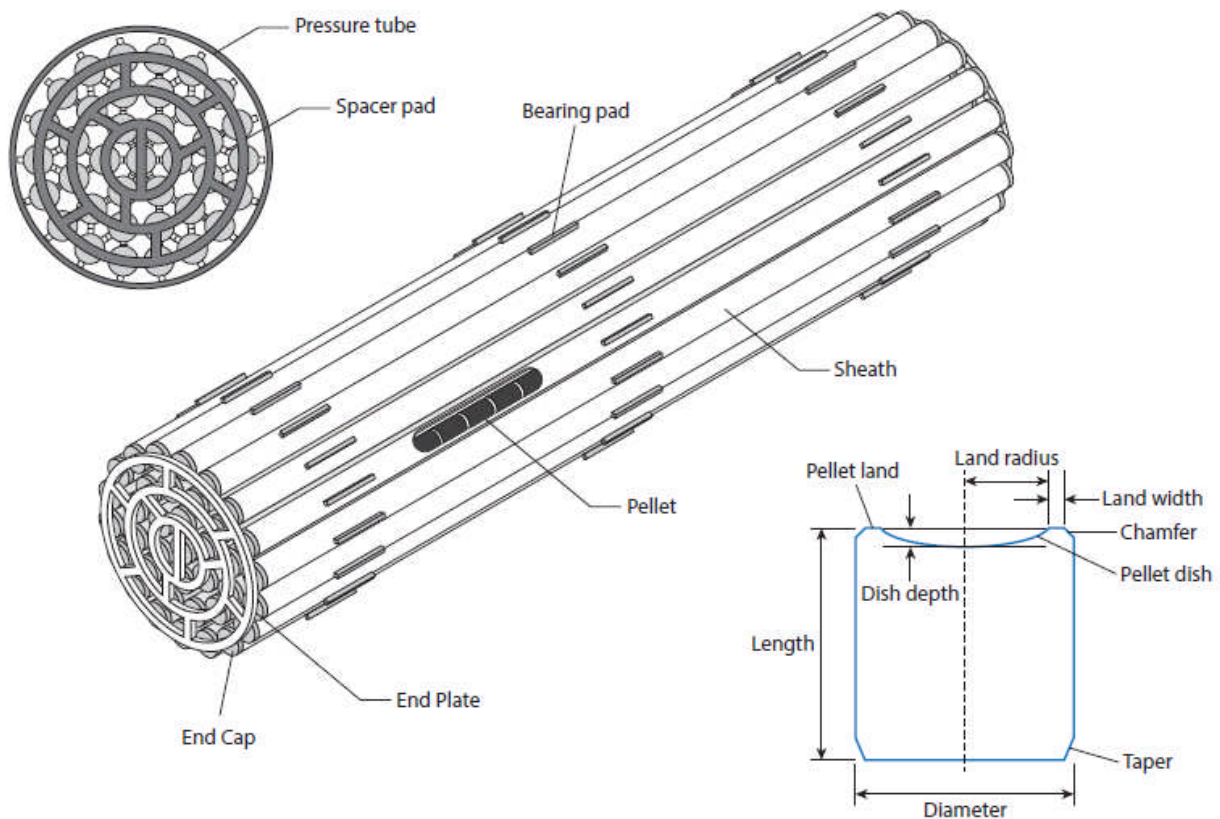


Figure 1 37-element CANDU fuel bundle

Broad overviews of fuel design have been provided in earlier chapters. The focus in this chapter is on the natural-uranium fuel used in current CANDU reactors, using the CANDU-6 reactor for illustration. Chapter 18 covers alternative fuel cycles that have also been considered for application in the CANDU reactor. Chapter 18 also covers, albeit briefly, some aspects of fuel manufacturing, including uranium mining, as part of a discussion on the natural uranium fuel cycle. Chapter 19 describes long-term storage and disposal of irradiated CANDU fuel. Discussion of

radiological hazards is beyond the scope of this chapter and is addressed in another chapter.

2 Overview

Before we can understand the science that underlies fuel integrity and therefore the chosen design, it is important to obtain sufficient background about the operating conditions for which nuclear fuel must be designed and the specific design that has been chosen to operate in them. These factors, in turn, determine which specific scientific disciplines are pertinent to fuel integrity.

2.1 Operating Environment

This section describes certain key illustrative (but not necessarily comprehensive) operating conditions that have major impacts on design choices for fuel and the science that underpins its performance in the reactor.

- **Power Intensity:** CANDU fuel produces a large amount of power in a small space. In a length of approximately 0.5 m, a fuel element some 13 mm in diameter produces, at its peak, some 30 kW. In comparison, a typical household electrical heater produces approximately 1 kW of heat when it is red hot. Therefore, nuclear fuel is 30 times more intense than the household electrical heater. This high heat intensity is a principal source of thermal and related challenges in nuclear fuel.
- **Coolant Temperature:** Reactor coolant is at high temperature—about 300° Celsius. This leads to concerns such as corrosion, hydriding, and creep in metals. Corrosion is also influenced by coolant chemistry. Corrosion and hydriding reduce the capability of Zircaloy to carry loads.
- **Coolant Velocity:** Coolant flows in the pressure tube at high velocity—approximately 10 m/s, or about 36 km/h—and at times this flow is turbulent. This leads to high drag loads and also to a potential for vibration, fatigue, and fretting.
- **Embrittlement:** Processes such as fast neutrons and hydrogen/deuterium picked up from corrosion tend to embrittle many metals and alloys. Therefore, shortly after insertion in the reactor core, fuel's structural materials have a much diminished capacity to resist tensile strains. These phenomena are important sources of microstructural contributions to structural challenges.
- **Fission Products:** Fission reaction results in solid and gaseous fission products. These fission products have a larger volume than the original uranium, and their higher volume must be accommodated. Gaseous fission products increase the internal pressure on Zircaloy, and if excessive, this pressure can crack the Zircaloy. In addition, some fission products are corrosive and can aggravate the structural challenges from mechanical loads, especially in materials that become embrittled during irradiation.
- **Fuel Management:** Natural uranium fuel results in relatively low excess neutronic reactivity; therefore, a CANDU reactor requires frequent addition of new fuel to maintain reactivity (see the earlier chapters on physics). For this reason, a CANDU reactor is refueled on an almost daily basis. Shutting down the reactor every day for refuelling would have a major impact on the total power produced by the reactor. Therefore, CANDU reactors are refueled while they are operating at full power. During on-power fuelling, the reactor coolant carries the new fuel bundle into the C6 fuel channel until it hits an existing bundle in the channel. Therefore, the new as well as the old fuel bun-

dles—the latter potentially more brittle—need to withstand impact loads. On-power fuelling also means that some irradiated fuel bundles are moved from a low-power axial position in the channel to (or through) a higher-powered axial location. This can lead to power-ramp challenges, as described in Section 8.

- **Refuelling:** The fuel bundle is loaded and unloaded on-power, remotely, through tight spaces, through bends, and sometimes through interrupted (discontinuous) supports. These aspects require tight dimensional control, good dimensional stability, reasonable flexibility, and allowances for wear.
- **Power Manoeuvring:** The reactor may be required to change its power level periodically to respond to grid demand. Periodic changes in the power extracted from the fuel add another dimension to fatigue considerations.
- **Long Duration:** A C6 fuel bundle stays in the reactor core for six months to two years. Therefore, the challenging conditions described above must be endured continually for long periods.

2.2 Fuel Design

Fuel is designed to address the operating conditions described above. Each fuel channel of a C6 reactor contains 12 fuel bundles.

Figure 1 shows a typical C6 fuel bundle. Each fuel bundle is made up of 37 fuel elements. Each fuel element consists of a thin cylindrical tube called a sheath, which is made of Zircaloy-4. The sheath encloses about 30 cylindrical pellets of UO_2 . A thin coating of a graphite-based compound (called CANLUB) is applied to the inside surface of the sheath to mitigate the harmful effects of power ramps, as described later in Section 8. Each fuel element is sealed at both ends by endcaps that are welded to the sheaths; these welds are called "closure welds". Endplates hold the fuel elements together in the geometric configuration of a fuel bundle. The endplates are welded to the fuel elements; these welds are called "assembly welds". Spacing between individual fuel elements is maintained using spacer pads. Spacing between the fuel bundle and the pressure tube is maintained by bearing pads. The bearing pads and the spacer pads are brazed to the fuel sheaths [Page, 1976; Gacesa *et al.*, 1983].

Figure 1 also shows some key aspects of the internal design of a fuel element. The axial profile of the pellet contains a dish to accommodate thermal expansion of the pellet that occurs because of high temperature during irradiation. To make it easier to insert the pellets into the sheath, (a) a diametric clearance is provided between the pellets and the sheath, and (b) chamfers are provided in the pellets. Axial clearance between the pellet stack and the two endcaps limits or even prevents axial interference between the two. A cavity in the endcap provides space to store fission gas produced during irradiation.

The following are key rationales for some of the chosen features:

- **Subdivision of the Bundle:** As one illustrative example, a choice was made to subdivide the uranium in the fuel bundle into a number of fuel elements. This permits the coolant to be near the source of the heat at many locations, leading to lower UO_2 temperature and reduced threats from many thermally driven damage mechanisms. At the same time, however, we should avoid excessive subdivision in the form of significantly more numerous but much smaller fuel elements along with additional spacer pads and bearing pads. The latter approach would add zirconium to the bundle, which would, among

other effects, increase parasitic absorption of neutrons; increase fabrication cost; provide additional resistance to flow and hence require bigger and costlier pumps to generate the same flow of reactor coolant; lead to greater potential for fatigue and fretting due to lower resistance of the smaller fuel elements to flow-induced vibrations; and exhibit higher propensity for creep sag of the smaller fuel elements, which could potentially lead to jamming of the fuel bundle in the channel. Increased subdivision also adversely impacts the neutronic-thermal-hydraulic interaction during accidents (coolant void reactivity), and, taken to the extreme, a much smaller element diameter would reduce the available surface area and decrease the efficiency of heat removal by the coolant. Hence, a judicious balance must be struck regarding the degree of subdivision.

- Circular Cross Section of Fuel Elements: As a second illustrative example, the circular cross section of the fuel elements reduces the stress concentration that would otherwise be introduced by non-circular cross sections. This increases the mechanical strength of the fuel elements to resist in-reactor loads.
- Ceramic, High-Density UO₂: A large amount of heat is generated in the uranium fuel under high external coolant pressure; therefore, the uranium must be in a form that will transmit heat efficiently and maintain structural integrity. Ideally, uranium would be used in a metallic form (e.g., uranium-aluminum alloy) to promote better heat transfer. However, uranium metal has two undesirable characteristics: (1) if a fuel sheath were to rupture and hot water from the coolant were to penetrate the fuel element, uranium metal would oxidize rapidly and lose its strength; and (2) uranium metal is also dimensionally unstable because of its anisotropy. Hence, uranium in the form of UO₂ is a good compromise. Although the low thermal conductivity of UO₂ leads to high temperatures in the fuel, its high melting point (about 2840°C) provides a large tolerance to melting. Maximizing the density of UO₂ leads to (1) higher fissile content in the element, hence more energy; (2) improved thermal conductivity and hence lower temperature; and (3) reduced in-reactor densification and hence higher dimensional stability.
- Zircaloy-4: Unlike the enriched uranium used in other types of reactors, CANDU reactors use natural uranium. The latter has much less ²³⁵U to undergo fission. Therefore, to sustain the chain reaction, it is essential that neutrons be conserved and that absorption of neutrons by structural materials be minimized. For this reason, the structural components are made from Zircaloy-4, which has a relatively small cross section for neutron absorption. In addition, the structural components are kept as thin as possible, including sheaths that are allowed to collapse if needed under operating pressure and temperature. Zircaloy-4 also has high corrosion resistance, which is important considering the high temperatures and the long residence periods in the reactor. Finally, Zircaloy-4 also has suitable mechanical properties.
- Thin Collapsible Sheaths: As a fifth illustrative example, the sheaths on CANDU fuel are purposely kept very thin, mainly to conserve neutrons. Another benefit of a thin sheath is that it can collapse diametrically under the operating pressure and temperature of the coolant. This improves heat transfer from the pellet to the coolant, which in turn lowers pellet temperature and reduces fission gas release. At the same time, the sheath must be strong enough to carry the in-reactor loads and to avoid forming overly sharp ridges (called longitudinal ridges, described in more detail in a later section of this chapter) which can fail by overstrain or by fatigue.
- Helium Filling Gas: To minimize damage from several mechanisms such as melting, fis-

sion gas pressure, and environmentally assisted cracking, the operating temperature of the pellet should be kept as low as reasonably achievable. Towards that end, empty spaces within a fuel element are filled with gas that has high thermal conductivity. This is called *filling gas*, and helium, or helium mixed with argon and air, is generally used for this purpose. Another advantage of helium is that it has very small atoms that can escape through small faults in joints: if a fuel element is not perfectly sealed by the endcaps during manufacturing, escaping helium can be detected by appropriate sensors during fuel fabrication.

- **Internal Shapes and Spaces:** Many internal shapes and spaces are carefully chosen to balance a number of conflicting objectives, e.g., to reduce stresses, to provide space for expansion during irradiation, to provide space to store fission gases produced during irradiation, and to promote large-volume, automated, low-cost production. Some such features include the pellet profile, the profile of the sheath/endcap junction, the endcap profile, the diametric clearance between the pellets and the sheath, and the axial clearance between the pellet stack and the endcaps. Several of these aspects are further elaborated upon in later sections of this chapter.
- **Manufacturing:** Some features are driven primarily by considerations of automation in manufacturing, e.g., resistance welding of endcaps and sheaths and brazing of pads. Both processes enable fast throughputs. Chapter 18 provides additional details of some aspects of fuel manufacturing.
- **Ease of Handling:** The length of the bundle was chosen primarily to facilitate on-power refuelling, although both the length and weight of the bundle have ergonomic advantages; one individual can lift and carry the bundle by hand.
- **Fuel Management:** Some important considerations in fuel management are: (a) to maintain neutronic reactivity at the desired level; (b) to achieve reasonable burnup; and (c) to avoid defects due to power ramps. The last aspect is discussed in more detail in a later section.

These configurations were chosen to facilitate the primary objectives of the fuel bundle: to produce heat, to maintain its geometry so that the coolant can carry the heat away, to ensure in-reactor integrity of the fuel elements and the fuel bundle, and to do all this consistently over a lengthy period.

In several other ways as well, the chosen features reflect careful balances among many conflicting requirements, processes, and forces. Fuel design is a complex multidisciplinary optimization process involving reactor physics, thermal-hydraulics, heat transfer, structural mechanics, microstructural processes, geometric stability, and interfacing systems, all under normal, off-normal, and accident conditions.

The choices described above—thin structural materials, high operating temperatures, axial movement of the fuel bundle during on-power fuelling, large in-reactor mechanical forces, and material degradation due to irradiation—all combine to pose unique and significant challenges to the in-reactor integrity of CANDU nuclear fuel under normal operating conditions. An overview of these challenges is given in the next section.

2.3 In-Reactor Challenges

The major challenges to fuel's in-reactor integrity can be grouped into three categories: (1)

thermal challenges, (2) mechanical challenges, and (3) compatibility challenges.

Thermal challenges, if excessive, can potentially cause melting in the pellet or in the structural materials (mainly Zircaloy). Pellet melting can result in (a) escape of additional fission gas from the UO_2 matrix into the pellet-to-sheath gap and (b) thermal expansion of the pellet, causing the sheath to rupture. This combination can send additional radioactive fission products into the coolant. Excessive amounts of radioactive fission products in the coolant could increase the radiological hazard to the health of station staff.

Excessive mechanical damage can potentially cause holes, cracks, or breaks in structural materials, with consequences similar to the thermal challenges described above.

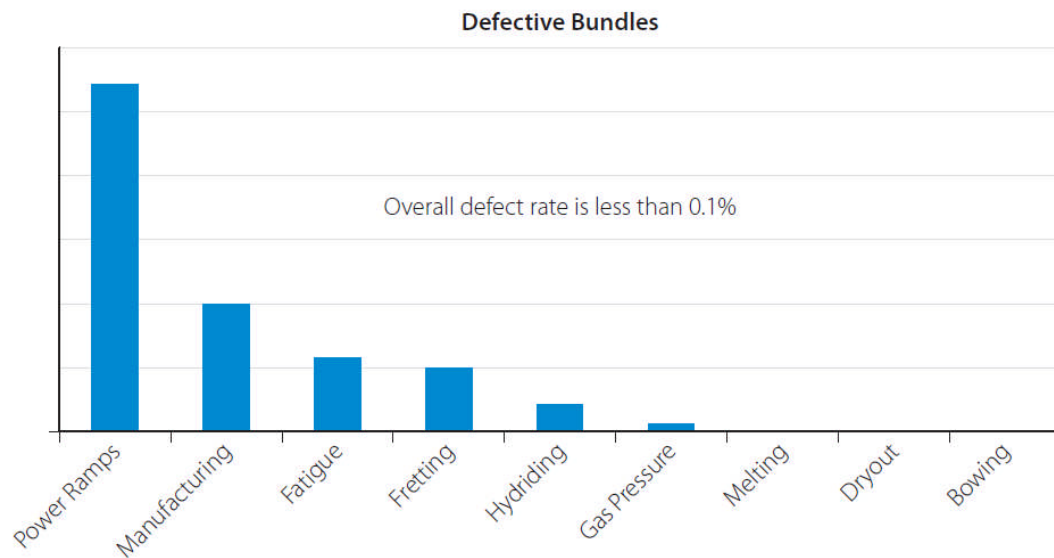
Incompatibility can potentially cause the fuel bundle to jam inside the reactor or in its accessories such as fuel handling equipment, interfering with its proper insertion or eventual removal. Incompatibility can also potentially harm neighbouring or interfacing components through processes such as crevice corrosion.

For these reasons, a major objective in fuel design is to limit the extent of damage from the mechanisms just described. Doing so requires, among other things, assessments of non-linear heat transfer, non-linear stress analyzes, and microstructural processes.

All damage mechanisms are under sufficient control in current CANDU fuels. In most mature CANDU cores, fuel defects typically occur in less than one bundle per year and tend to be caused mostly by fretting due to debris.

The defect rate of CANDU fuel is remarkably low. During 2007–2008, the International Atomic Energy Agency (IAEA) conducted a world-wide survey of fuel defect rates from 1994 to 2006 [IAEA, 2010]. World-wide, water-water energy reactors (WWERs) were found to have a fuel defect rate of 94 defective fuel elements per million discharged (also called ppm, or parts per million). The fuel defect rate was 87 ppm in pressurized water reactors and 65 ppm in boiling water reactors. In comparison, fuel in Canada had a defect rate of 3.5 ppm. The Canadian fuel defect rate is very acceptable—almost in the range of impurities found in most substances—and much lower than for other types of nuclear fuels. This low rate confirms the basic soundness of the practices built into all major aspects of Canadian fuel, from research to development, to design, to fabrication, to operation, and to feedbacks among them.

Nevertheless, several defect excursions have occurred in the past, and it is illustrative to examine the historical causes of significant fuel defects. Figure 2 shows readily available illustrative data on fuel bundles which have been damaged, mostly in defect excursions in power reactors during the first three decades of commercial nuclear power, although the figure also includes some data that would not strictly be considered to represent a major defect excursion.



Note: Above data exclude failures due to debris

Figure 2 Causes of defects in CANDU fuel (1967–1996)

The International Atomic Energy Agency has defined a “defect excursion” as one in which 10 or more fuel bundles fail within a 12-month period [IAEA, 2010]. Figure 2 does have limitations: it focusses on defects related to design and/or operation, mostly in Canada, and it excludes defects due to fretting by debris. One can postulate that for any given damage mechanism, the amount of damage is an indicator of how close its failure threshold is to the operating conditions—the closer one operates the fuel to the defect threshold of a specific damage mechanism, the higher will be the likelihood of damage from that mechanism. Figure 2 demonstrates that in the past, power ramps have been a dominant damage mechanism in CANDU fuels.

The underlying science of the relatively more important challenges to fuel integrity is described in later sections of this chapter. Table 1 provides some illustrative design data for C6 fuel. Likewise, Table 2 provides some illustrative data for the physical, thermal, and mechanical properties of CANDU fuel; these can be used for illustrative calculations of fuel performance.

Table 1 Illustrative design data for C6 fuel

[Major Source: Nuclear Engineering International, September 2006]

Parameter	Value	Parameter	Value
Number of elements (rods) per bundle (assembly)	37	Element length (mm)	493
Peak linear fuel element rating (kW/m)	57	Element outside diameter (mm)	13
Average discharge burnup of fuel bundle (MWh/kgU)	170	Sheath (clad) thickness (mm)	0.4
Maximum residence period in the reactor (days)	700	Pellet outside diameter (mm)	12
U weight per bundle (kg)	19.2	Pellet length (mm)	16
Zr weight per bundle (kg)	2.2	Pellet density (g/cm ³)	10.6
Overall bundle length (mm)	495	Endplate width, outer ring (mm)	4.9
Overall maximum bundle diameter (mm)	102	Endplate thickness (mm)	1.6
Average sheath temperature (°C)	340	Diameter of assembly weld (mm)	4

Table 2 Illustrative data for fuel assessments

Parameter	Value	Parameter	Value
UO ₂		Zr-4	
Thermo-Physical Data			
Theoretical density (g/cm ³)	10.97	Density (g/cm ³)	6.56
As-fabricated density (g/cm ³)	10.6	Thermal conductivity at 300°C (W/(m.k))	16.4
Thermal conductivity at 1000°C (W/(m.K))	2.8	Specific heat capacity at 300°C (J/(kg.K))	327
Specific heat capacity at 1000°C (J/(kg.K))	328	Melting point (°C)	1850
Melting point at zero burnup (°C)	2840	Sheath-to-coolant heat transfer coefficient (kW/m ² K)	50
Pellet-to-endcap heat transfer coefficient (kW/m ² K) (at high power, hard contact, low burnup)	1	Pellet-to-sheath heat transfer coefficient (kW/m ² K) (at high power, hard contact, low burnup)	80
Mechanical Data			
Young's modulus at 1000°C (GPa) (at 98% theoretical density)	190	Young's modulus at 300°C (GPa)	80
Poisson's ratio	0.316	Shear modulus (GPa)	27
Yield strength at 1000°C (MPa) (for grain size of 25 µm)	180	Poisson's ratio	0.37
Coefficient of linear thermal expansion (µm/(m.K)) (at 1000°C)	12.5	Yield strength at 300°C (78% cold worked and stress relieved at 510°C)	274
		Coefficient of linear thermal expansion (µm/(m.K)) (diametric, at 300°C)	6.72

3 Power and Burnup

Recall from the earlier chapters on physics that the heat output of a fuel element is usually expressed in kW/m. The energy produced by a fuel element per unit mass is called “burnup”. It is also customary to use burnup as an indicator of irradiation time, although strictly speaking, time is equal to energy divided by power. In the CANDU fuel community, burnup is usually measured in MWh/kgU. In other types of fuel, e.g., in PWRs and BWRs, fuel burnup is usually measured in GWd/tU. 1 GWd/tU equals 24 MWh/kgU.

Sometimes “atomic percent” is also used as a unit of burnup. It measures the ratio of the number of fissions to the initial number of uranium atoms. As a working rule, 1 atomic percent equals 240 MWh/kg U.

Exercise: A fuel element is operating at 60 kW/m and contains UO₂ cylinders of 12 mm diameter. What will be the fuel burnup after 30 days?

One meter of this fuel element contains a UO₂ volume of 113 ml. Assuming a UO₂ density of 10.6 g/cm³, the mass of UO₂ is 1.2 kg. In UO₂, 88% is U. Therefore, one meter of this fuel element contains $(1.2 * 0.88) = 1.06$ kg of U. This fuel element is producing 60 kW; therefore, in 30 days, it produces $(60 * 720/1000) = 43$ MW•h. Therefore, its burnup is $(43/1.06) = 41$ MW•h/kgU.

This example illustrates that a typical CANDU fuel element operating at 60 kW/m accumulates about 41 MW•h/kgU of burnup every month.

Recall from the earlier physics chapters that in a CANDU channel, the flux can change significantly from one channel to another and from one axial location in a channel to another. Also recall from the chapters on physics that to maintain reactivity, some fuel bundles are periodically moved from one axial location in the channel to another. These factors produce a variety of power histories in any given bundle.

Figure 3 shows two illustrative power histories for CANDU fuel. The first is called a “declining” power history and would be experienced by a fuel bundle that is loaded in a central axial location of a C6 fuel channel. The second includes a “power ramp” and is experienced by CANDU fuel which is initially loaded in a low-flux axial location of the channel and later shifted to a location of higher flux.

Different types of power histories have different impacts on fuel performance. For example, an element with a declining history generally experiences high power for a long period, which usually results in relatively high gas pressure in the fuel element. On the other hand, a ramped history exposes the fuel element to relatively high risk of “environmentally assisted cracking”. These aspects are illustrated further in later sections.

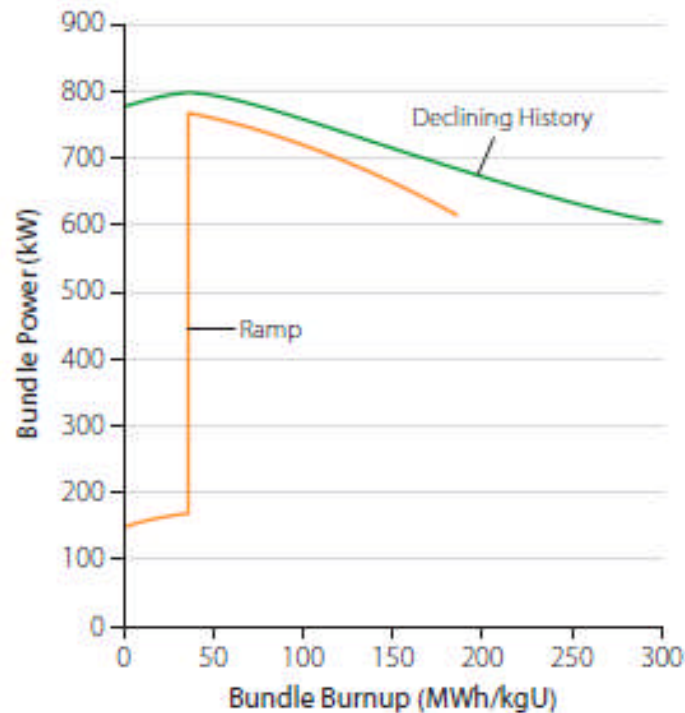


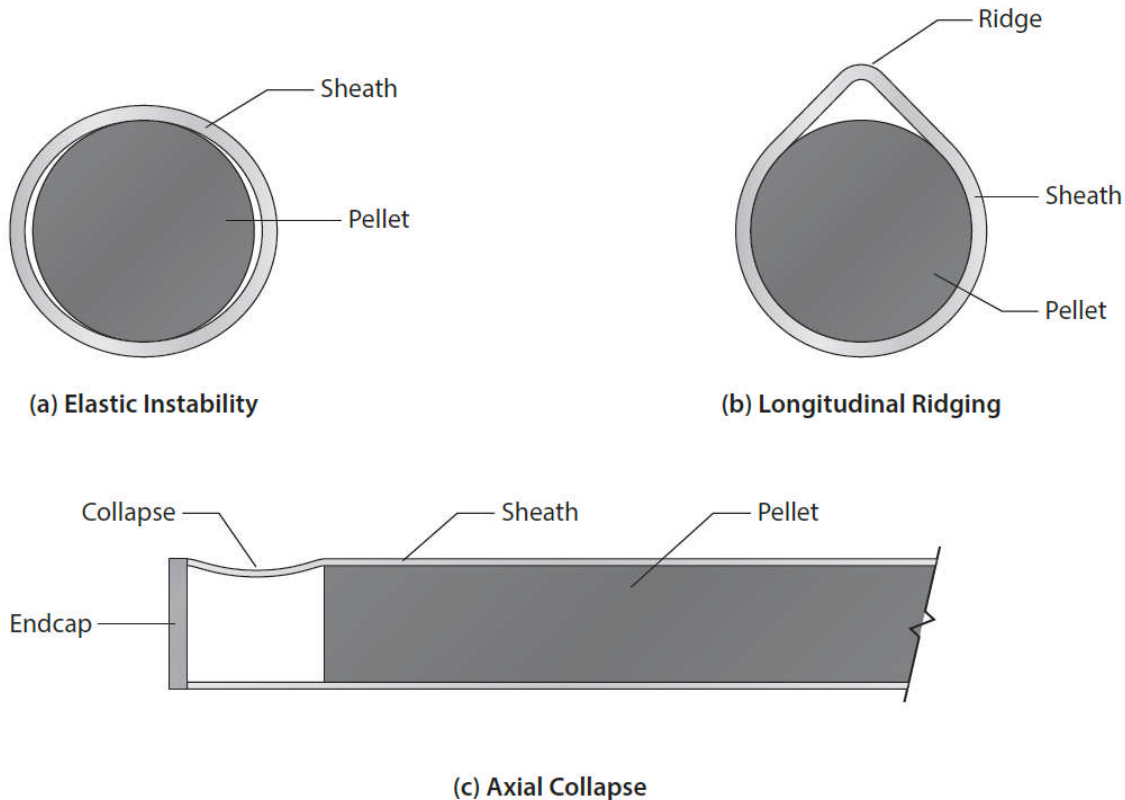
Figure 3 Illustrative power histories

4 Collapsible Sheaths

To minimize unnecessary parasitic absorption of neutrons, CANDU fuel sheaths are kept very thin—so thin that coolant pressure induces high compressive hoop stresses in them. At sufficiently high compressive hoop stress, the sheath will lose its elastic stability and collapse diametrically inwards into the diametric gap between the sheath and the pellet until it is supported by pellets. Figure 4(a) illustrates this phenomenon.

This collapse improves contact between the pellet and the sheath and therefore improves heat transfer between them. This, in turn, lowers pellet temperature and reduces thermally driven processes. Some such processes, such as diffusion and release of fission gas, decrease exponentially with reduced local temperature. Therefore, even a modest decrease in local pellet temperature leads to a disproportionately large reduction in these processes. For this reason, designers of CANDU fuel prefer to promote diametric collapse of the sheath.

At the same time, excessive diametric or axial collapse can risk sheath failure from overly high local strains. These conditions are called longitudinal ridging and axial collapse respectively (see Figures 4(b) and 4(c)) and must be avoided. Therefore, a delicate balance must be struck between promoting sufficient collapse to improve pellet-to-sheath heat transfer and avoiding overstrain due to excessive collapse. This trade-off is explained in the following sections.



Note: Shapes have been exaggerated for clarity

Figure 4 Sheath collapse: forms and stages

4.1 Diametric Collapse

Elastic instability in a thin circular cylinder can be calculated from Bryan's equation [Bryan, 1888]:

$$P = E (t/r)^3 / [4(1-\nu^2)],$$

where P is the differential pressure (= coolant minus internal), E is Young's modulus, t is thickness, r is radius, and ν is Poisson's ratio.

Exercise: Consider a fuel sheath with the following properties: diameter, 13 mm; thickness, 0.4 mm; Young's modulus, 80 GPa; and a Poisson's ratio of 0.37. Its collapse pressure is $80,000 * (0.4/6.5)^3 / (4 * (1 - 0.37^2)) = 5.4$ MPa.

In other words, the sheath just described will become elastically unstable when the differential pressure (coolant minus internal) exceeds 5.4 MPa. By comparison, the coolant pressure is 10 MPa. Therefore, when a C6 fuel element is first loaded into the reactor, the sheath will collapse elastically into the diametric gap.

Internal gas pressure builds up during irradiation (see Section 6). If the internal pressure in the fuel element exceeds about $(10 - 5.4) = 4.6$ MPa, the differential pressure will drop below the collapse pressure. The sheath will then no longer have much circumferential contact with the pellet, unless by then creep has converted sufficient elastic strain into permanent plastic deformation.

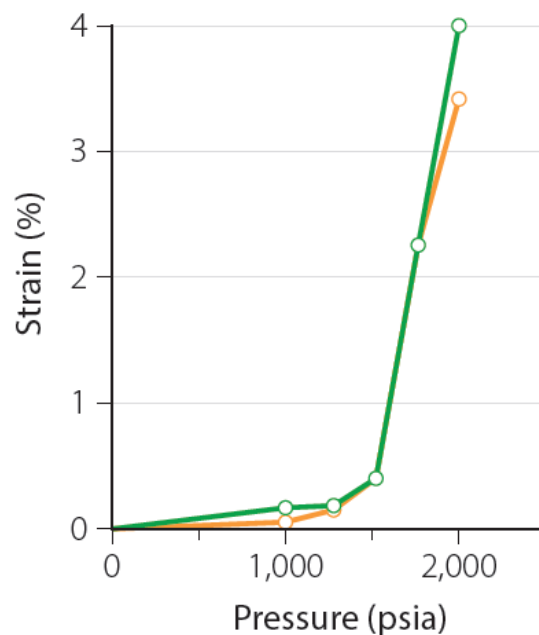
Improved heat transfer from diametric collapse is comparatively more important at high power

because fission gas diffusion increases exponentially with higher temperature. At the beginning of life, the internal pressure is low, the sheath is elastically unstable, the sheath is in contact with the pellet, and pellet-to-sheath heat transfer is good. This helps reduce the diffusion and release of fission gas. By the time internal gas pressure builds up sufficiently to provide elastic stability to the sheath, the element rating has usually decreased with burnup. Therefore, by then, good heat transfer is not as critically important.

4.2 Longitudinal Ridging

If the coolant pressure increases well past the collapse pressure, eventually the sheath starts to wrap itself around the pellet, as shown in Figure 4(b). This eventually creates a sharp ridge that runs along the length of the sheath, called a longitudinal ridge. Depending on how sharp the ridge is, the tip of the ridge can experience high bending strain. In an experimental irradiation, fatigue cracks eventually developed at longitudinal ridges. Some experts have also postulated that hydrogen in the sheath can migrate preferentially to longitudinal ridges, potentially hydriding and thereby embrittling the sheath at that location. For these reasons, strain at longitudinal ridges must be controlled to reasonable levels.

Figure 5 shows a typical development of permanent strain at the tip of a longitudinal ridge when pressure is increased. The two curves in this figure illustrate typical scatter in two different test specimens in this specific experiment.



[Courtesy of COG]

Figure 5 Illustrative permanent strain at the tip of a longitudinal ridge

Initially, the strain increases rather gradually. Beyond a critical strain, however, a further increase in pressure increases the sheath strain fairly rapidly. The point at which this occurs is called the critical strain and has been experimentally found to be 0.5%. It is good practice to design CANDU fuel to stay below this strain value at the longitudinal ridge. Fuel designed in this way has never exhibited sheath failures at longitudinal ridges.

Experiments have established that the following parameters are relatively more important in influencing ridge strain: differential pressure, diametric clearance, sheath thickness, sheath diameter, yield strength, and Young's modulus.

4.3 Collapse into the Axial Gap

If the sheath is too thin, or if the axial gap is too long, the sheath can potentially collapse into the axial gap, as shown in Figures 4(c), 6(a), and 6(b). Such a collapse has the potential to crack the sheath, and therefore it is good engineering practice to avoid it.

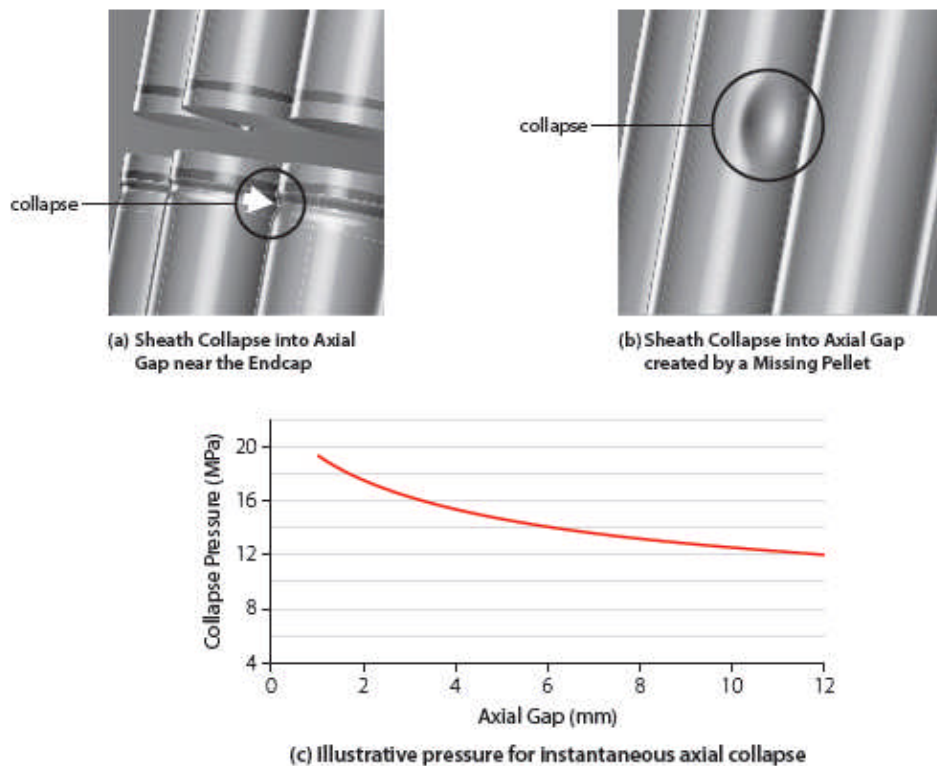


[Figure (c) courtesy of COG]

Figure 6 Collapse into axial gap

The following major parameters influence axial collapse: differential pressure, length of the axial gap, radius and thickness of the sheath, and the yield strength, Young's modulus, and Poisson's ratio of the sheath material.

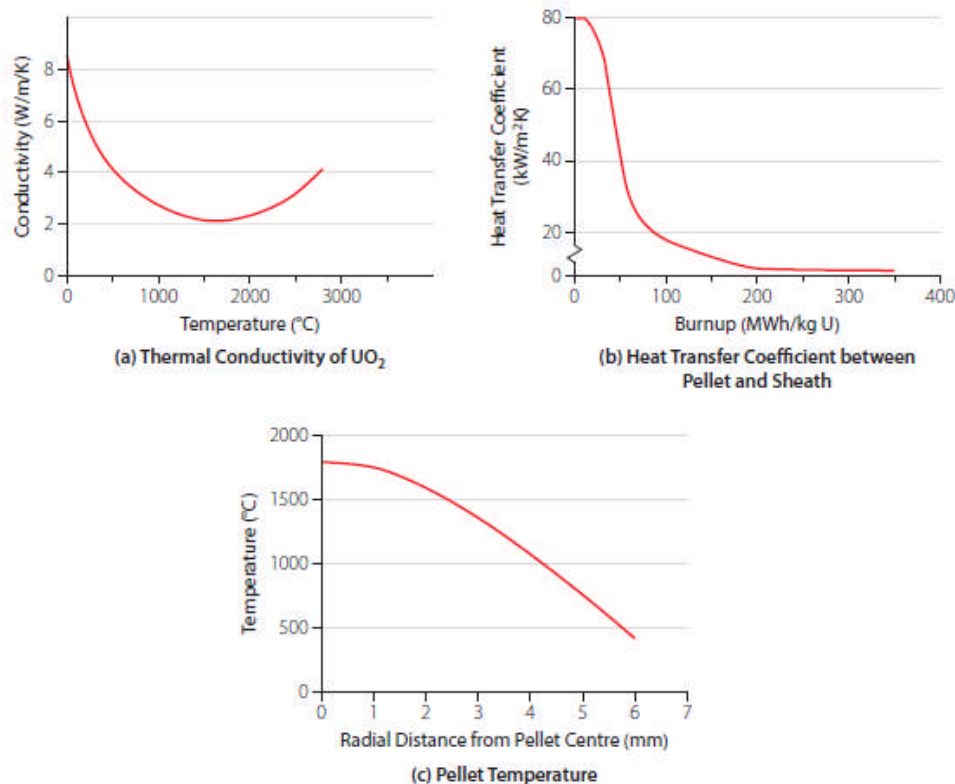
Figure 6(c) shows an illustrative calculation for instantaneous axial collapse in 37-element fuel. Creep collapse can potentially occur at a lower pressure than the instantaneous collapse pressure.

In CANDU fuel, axial collapse has been observed only under unusual situations such as absence of a large part of a pellet or an excursion to unusually high temperature in experimental fuel.

5 Thermal Performance of Fuel

High temperatures in the UO_2 pellet and in the Zircaloy sheath are important drivers for many damage mechanisms. Other chapters discuss the equations that can be used to calculate temperature distributions inside the fuel element.

Table 2 and Figure 7 provide some illustrative data that can be used to assess the thermal performance of fuel.



[Source: Tayal *et al.*, 1987]

Figure 7 Illustrative heat transfer and pellet temperature in a fuel element

Some parameters are not constant, but depend on other parameters. For example, Figure 7(a) shows that the thermal conductivity of UO_2 depends on local temperature. Likewise, the heat transfer coefficient between the pellet and the sheath changes significantly with time, as shown in Figure 7(b), because of changes during irradiation in factors such as the interface pressure between the pellet and the sheath and the volume and composition of fission and filling gases within the fuel element. In such cases, Table 2 lists an average representative value that can be used for illustrative calculations.

Figure 7(c) illustrates a typical local temperature profile across the pellet radius. Note that (a) the temperature distribution is approximately parabolic, (b) the temperature at the centre of the pellet is about 1,800 $^\circ\text{C}$, and (c) the temperature at the surface of the pellet is about 400 $^\circ\text{C}$. Needless to say, the absolute values of temperature depend on many parameters, including

element power; Figure 7(c) is merely an illustrative example.

The above absolute temperatures, as well the temperature gradient across the pellet radius, have significant consequences for fuel performance, as discussed in more detail later in this chapter.

6 Fission Gas and Internal Pressure

6.1 Overview

Each fission reaction produces fission products (fission fragments), as described in earlier chapters on physics. Some fission products are solid, whereas others are gaseous. These fission products accumulate over time. The gaseous fission products lead to internal pressure which, if excessive, can potentially create a hole in the sheath, either through mechanical overstrain or through environmentally assisted cracking. A hole can provide a path for radioactive fission products to leach into the coolant and to pose a radiological hazard to operating staff. For this reason, fission gas pressure must be controlled and limited to acceptably low values.

As noted earlier, CANDU fuel is designed to have collapsible sheaths to improve heat transfer to the coolant, which reduces pellet temperature, which in turn reduces the amount of fission gas that can escape from the pellet and contribute to gas pressure in the fuel element. In addition, through appropriate pellet shapes and clearances, empty space—called “open void”—is provided inside a fuel element to keep internal gas pressure below acceptable levels.

Over the years, CANDU reactors have maintained good control of fission gas pressure. In a rare instance, however, control of fission gas pressure was lost for a very brief period in the 1980s in a Bruce reactor in Ontario when unavailability of a fuelling machine prevented timely refuelling of a fuel channel. As a result, some fuel bundles resided in the core for longer durations than designed, resulting in excessive accumulation of fission gas and in high internal pressure. This in turn caused cracks in the sheaths of a few fuel elements. The internal gas pressure can be calculated using a model summarized below [Notley *et al.*, 1979].

Figures 8–14 show some processes pertinent to fission gas pressure. Fission produces gas uniformly within the grains of UO_2 . However, to exert pressure on the sheath, the gas must first reach the “open space” within the fuel element (Figure 8a). This is the space in the axial and diametric gaps, in the dishes, in the chamfers, in the cracks within the pellets, in the surface roughnesses of the sheath and of the pellets, and in the cavity of the endcap. The movement of gas from within grains to the open space is described below.

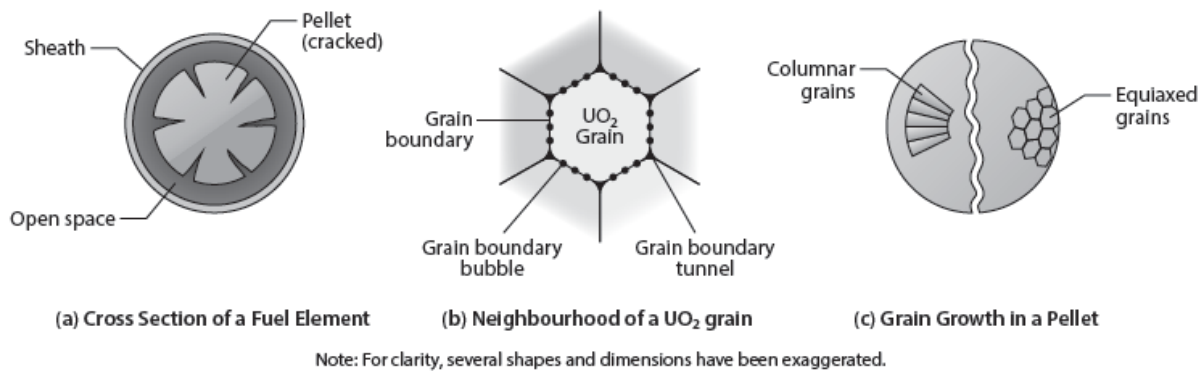
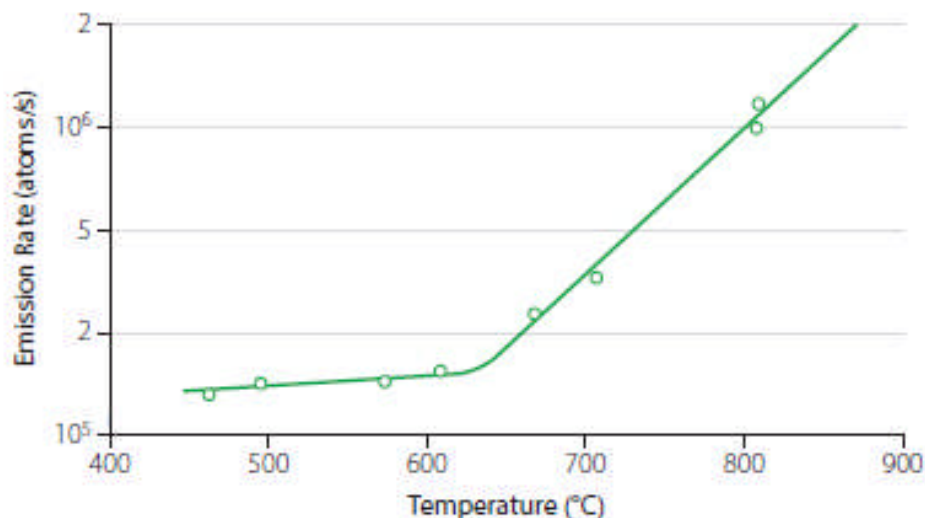


Figure 8 Terms for fission gas release

A number of processes are involved in transporting fission gas from within grains to the open voidage. They include knock-out, recoil, diffusion, grain boundary sweep, storage in grain boundary bubbles, growth of grain boundary bubbles, interlinkage of grain boundary bubbles, and venting of grain boundary bubbles. These are described in the following paragraphs.

Figure 9 is an illustrative example of the steady-state release rate of ^{88}Kr from a single crystal of UO_2 [Carroll *et al.*, 1965].



[After Carroll *et al.*, 1965]

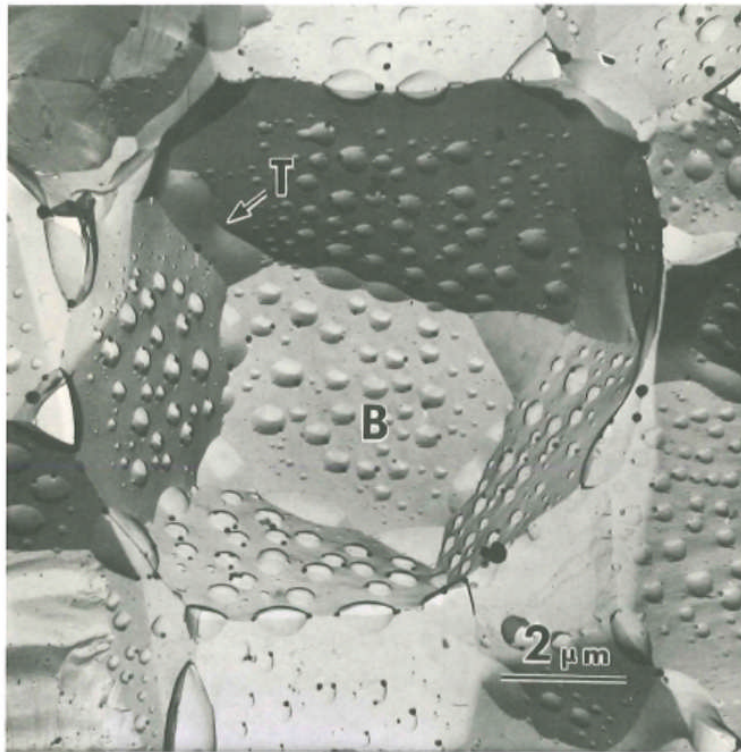
Figure 9 Steady-state release of ^{88}Kr from a single crystal of UO_2

Below about 625°C, two thermally-independent processes—recoil and knockout—make significant contributions to total release of fission gas. They are also sometimes called “athermal” release mechanisms.

Above about 625°C, the emission rate increases rapidly with temperature. This is due to diffusion, because diffusivity increases exponentially with temperature. This phenomenon is also sometimes called “thermal” release. If high fission gas pressure does occur in CANDU fuel, it is almost always driven primarily by thermal diffusion.

Fission gas is produced within grains. If the grain boundary acts as a sink, a gradient develops in the concentration of gas across the grain's radius. This concentration gradient drives the rate of diffusion from the grain to the boundary.

At the grain boundary, the gas accumulates in bubbles (Figures 8(b) and 10), which become progressively bigger as more gas reaches the grain boundaries.



B: Bubbles; T: Tunnels
[Source: Hastings, 1983]

Figure 10 Grain boundary bubbles and tunnels

In parallel, high temperature can also cause the grains to grow (Figures 8(c) and 11), either through equi-axial grain growth (Figure 12) or, at even higher temperatures, through columnar grain growth (Figure 13). The boundaries of the growing grains collect the gas that was previously contained in the areas swept by grain growth. This gas is added to the inventory of gas at grain boundaries. This process is called grain boundary sweep.

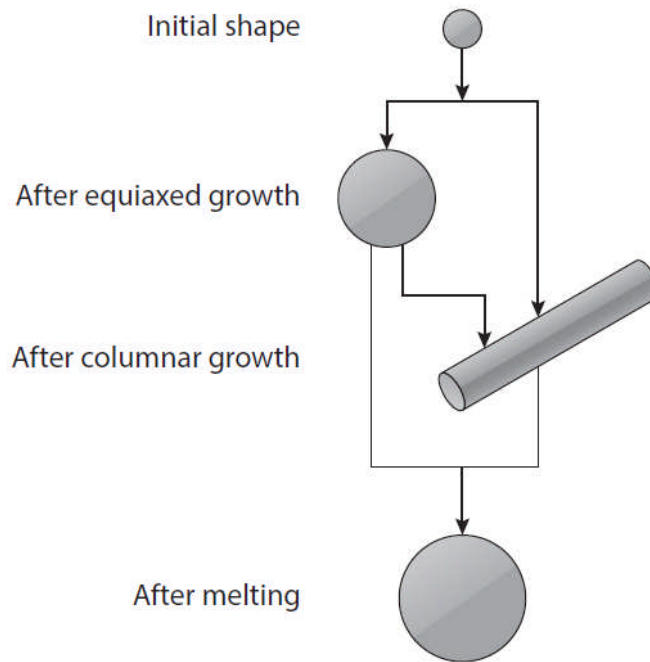


Figure 11 Changes in sizes and shapes of UO_2 grains during irradiation

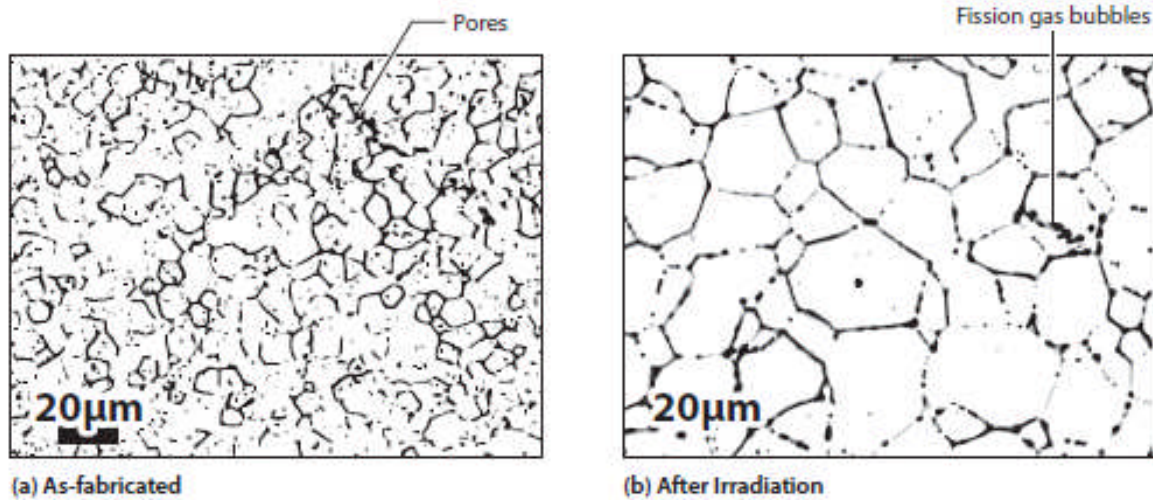
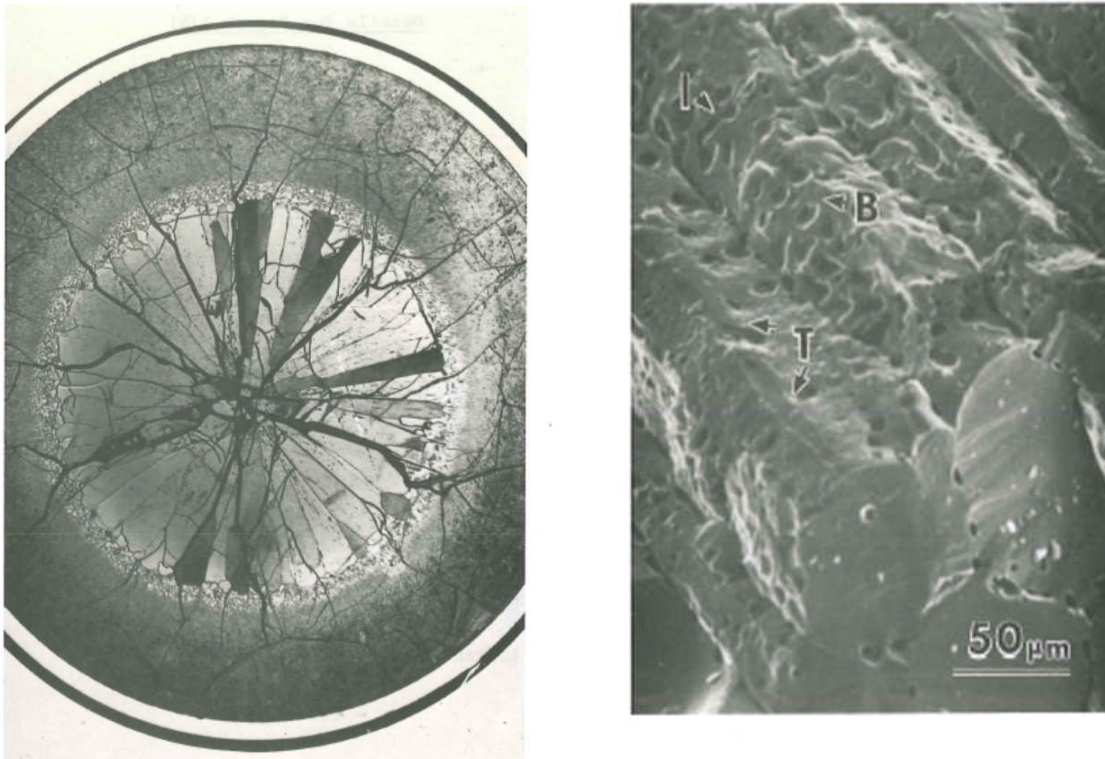


Figure (b) also shows fission gas bubbles at grain boundaries
[Source: Hastings, 1982]

Figure 12 Equiaxial grain growth



[Source: Hastings, 1983]

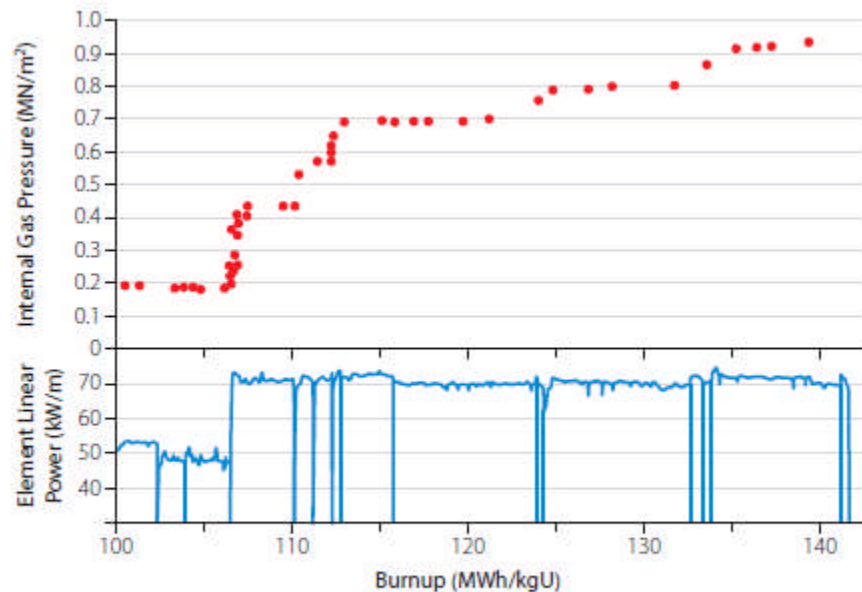
Figure 13 Columnar grain growth

As additional gas reaches grain boundaries, the grain boundary bubbles eventually become big enough to touch each other. This is called interlinkage. The volume contained within interlinked bubbles reflects the storage capacity of the grain boundary bubbles. Any gas that reaches the grain boundaries over and above the bubble capacity is called excess gas.

When fuel power changes, thermal expansions or contractions in the pellet create micro-cracks in the UO_2 ceramic. These provide a pathway for the excess gas in interlinked bubbles to vent to the open space between the pellet and the sheath. This can be deduced from Figure 14, which shows measurements of internal pressure during irradiation [Notley *et al.*, 1979].

Figure 14 shows that at high power, internal pressure does not change during constant-power periods, even though fission gas must be produced continually during these periods. Internal pressure increases only immediately after changes in power, suggesting that grain boundary gas escapes to the open space through interconnected micro-cracks formed upon changes in power.

Under the usual operating conditions in CANDU power reactors, only a small fraction (<10%) of the gas produced vents to the open space. Most of the gas stays tied up within the grains of UO_2 and in grain boundary bubbles.



[Source: Notley *et al.*, 1979]

Figure 14 Variation of internal gas pressure during irradiation

The process by which fission gas reaches the open space is called fission gas release. It increases rapidly with higher local temperature, and for a given temperature, it increases with burnup and with smaller grain size.

Later sections of this chapter will describe a simplified model to quantify the amount of fission gas that reaches the grain boundaries through diffusion.

6.2 Recoil

Recoil is one of the mechanisms that releases fission fragments outside the pellet. To a first approximation, fission fragments travel through UO_2 in a straight line. They lose energy as they encounter (primarily) electrons in the material. When the initial kinetic energy of the fission fragment has been fully dissipated in this process, the fission fragment stops as a fission product. This occurs in about $10\ \mu\text{m}$. However, if the fission fragment reaches a surface of the pellet before expending all its energy, it escapes the pellet. Therefore, recoil is a contributing factor in fission product release from near a surface of the pellet ($\sim 10\ \mu\text{m}$), especially at low temperature [Olander, 1976].

6.3 Knockout

Knockout is another athermal mechanism for fission product release that occurs at low temperature. As a fission fragment travels through the pellet, it may occasionally collide with nuclei of other atoms in the lattice. The latter are called “knock-ons”. Knock-ons are usually uranium or oxygen atoms in the fuel, but occasionally a knock-on can be a fission gas atom lodged in the lattice. A knock-on acquires kinetic energy from the collision, and it also travels in a straight line

and loses energy as it travels. A primary knock-on generally travels a distance of about 200 Å (Angstroms) before coming to rest. If the knock-on reaches a surface of the pellet before stopping, it escapes the pellet. If the knock-on was a fission fragment, this process results in release of fission products [Olander, 1976].

6.4 Diffusion of Fission Gas to Grain Boundaries

As noted earlier, diffusion is a key process that drives the fraction of produced gas that eventually reaches the open space at high operating power. This section discusses the rate of diffusion of stable gases to grain boundaries after a steady-state profile of gas concentration has been built across the grain. This can be calculated from Booth's model [Booth, 1957].

Grains of UO_2 are of irregular shape and size. Nevertheless, this calculation model postulates that gas diffusion out of grains can be approximated by assuming that the pellet consists of a collection of spheres of equal radii. The radius " a " of the equivalent sphere is equal to the average grain radius.

To calculate the leak rate at the grain boundary, we first need to know the gas concentration profile across the grain radius. Booth solved Fick's equation for diffusion in a sphere [Fick, 1855] assuming that the surface of the sphere was a sink. This results in a parabolic concentration profile:

$$c(r) = \frac{f\beta}{6D}(a^2 - r^2), \quad (1)$$

where c is the local concentration, r is the radial distance from the grain centre, a is the grain radius, f is the fission rate, β is the yield, and D is the diffusivity. Concentration means the number of nuclides per unit volume of the grain. By integrating the above equation, we can obtain the volume-average concentration c_{av} .

Diffusion due to a concentration gradient results in the following rate of nuclide flow per unit area of grain surface, q :

$$q = -D \frac{\partial c}{\partial r} \text{ at } r = a. \quad (2)$$

The leak rate $LEAK$ is defined as the rate of nuclide diffusion from the grains per unit grain volume. Therefore [Tayal *et al.*, 1989],

$$LEAK = -\frac{3}{a} D \frac{\partial c}{\partial r} \text{ at } r = a. \quad (3)$$

By differentiating Equation (1), substituting the results into Equation (3), and then substituting the expression for c_{av} into Equation (3), we get:

$$LEAK = \frac{15Dc_{av}}{a^2}. \quad (4)$$

Equation (4) describes the rate at which fission gas diffuses to the grain boundary during steady state.

6.5 Internal Gas Pressure

As noted earlier, internal gas pressure must be kept within acceptable levels to avoid overstrain

failures. Therefore, internal gas pressure is a consideration in selecting some details of the internal design of a fuel element, such as pellet shape and axial gap.

Internal gas pressure is driven by the combined volumes of filling gas and fission gas. These gases are stored in a variety of locations within a fuel element, e.g., in dishes, in pellet/sheath radial gaps, in axial gaps, in pellet cracks, and in surface roughnesses of the pellet. Furthermore, the local temperature at each storage location differs significantly because of the steep temperature gradients within the fuel element.

To calculate the internal pressure, one usually divides the fuel element into many regions, each with a nearly constant temperature. Then the ideal gas law is used to integrate the impacts on internal gas pressure:

$$p_1 v_1 / T_1 = p_2 v_2 / T_2, \quad (5)$$

where p , v , and T represent pressure, volume, and temperature respectively and subscripts 1 and 2 refer to two different states.

Exercise:

Consider a fuel element which was initially filled with 2 ml of helium at standard temperature and pressure (STP). During irradiation, 10 ml (at STP) of fission gas was released to the open space. Let us assume for simplicity that at operating power, the open space in the fuel can be divided into three zones of essentially constant temperature, each with a volume:

- 0.4 ml at 1,900 K;
- 1 ml at 1,500 K; and
- 0.6 ml at 1,000 K.

This fuel element's internal gas pressure can be calculated as follows. Recall that at STP, the temperature is 273 K and the pressure is 0.1 MPa. Therefore, corresponding to the filling gas volume of 2 ml at STP, the "voidage" (V/T) is $(2/273) = 0.00733$ ml/K.

On-power, the same gas is now stored at an effective voidage of $(0.4/1900 + 1/1500 + 0.6/1000) = 0.00148$ ml/K. In other words, the on-power voidage is about $(0.00148/0.00733)$, or one-fifth the off-power voidage. Therefore, from the ideal gas law, the on-power pressure of the filling gas is $(0.1 * 0.00733/0.00148) = 0.5$ MPa.

Including the fission gas, the total STP volume of gas is $(2+10) = 12$ ml. On-power, because 2 ml (STP) of filling gas develops a pressure of 0.5 MPa, 12 ml (STP) of filling gas plus fission gas will develop a pressure of $(0.5 * 12/2) = 3$ MPa.

7 Stresses and Deformations

A variety of mechanical and thermal loads and microstructural changes lead to in-reactor stresses, strains, and deformations in fuel. Excessive stresses and strains can in turn potentially result in a hole in the sheath or in the endcap, which can release radioactive fission products to the coolant. Excessive stresses or strains in the endplate can break it also, which may pose difficulties in discharging the fuel from the reactor. Excessive deformations can potentially jam the fuel in the channel, reduce local cooling, or damage surrounding components through, for example, crevice corrosion.

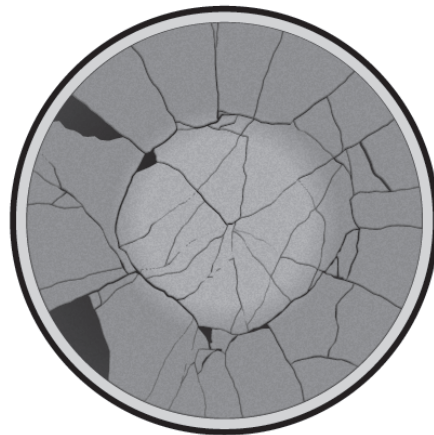
It would be unrealistic to operate fuel with zero stresses, strains, and deformations, and it

would be very expensive to limit these always to trivial values through massively over-conservative designs. At the same time, it is essential to keep them reasonably below harmful levels. Some such considerations are described in this section.

7.1 Thermal Stresses in Pellets

As noted in an earlier chapter, the radial temperature distribution in an operating fuel pellet is, to a first approximation, parabolic. The temperature gradient is steep, about 1800°C at the centre and about 400°C at the surface, over a radius of only about 6 mm.

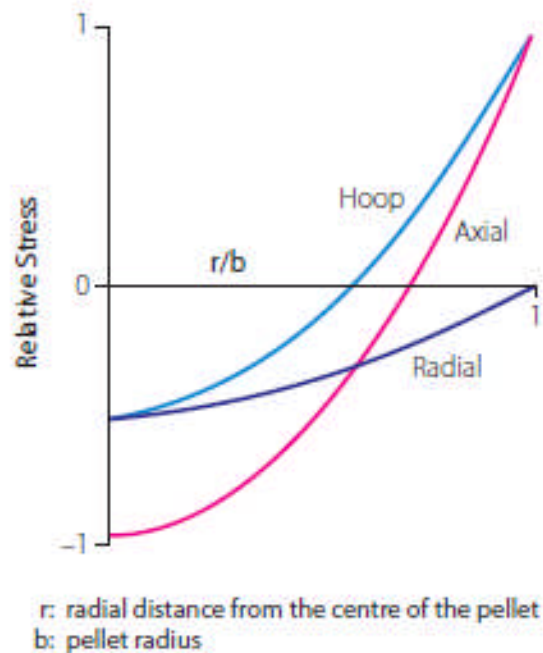
Think of a pellet as being made up of many concentric rings (or annuli). Thermal expansion is higher in the inner hotter rings and comparatively lower in the neighbouring, relatively cooler outer rings. Differential thermal expansions lead to dimensional misfits between neighbouring annuli, which in turn lead to stresses. For this reason, operating UO₂ pellets are often found with extensive radial cracks in their outer regions, as shown in Figure 15.



[Source: Hastings, 1983]

Figure 15 Typical cracks in a high-power pellet

Textbooks in mechanics provide a framework of equations which can be used to calculate thermal stresses in a cylinder experiencing parabolic temperature profile across its radius [e.g., see Timoshenko *et al.*, 1970]. Figure 16 illustrates a typical result.



[Courtesy COG]

Figure 16 Thermal stresses in a pellet

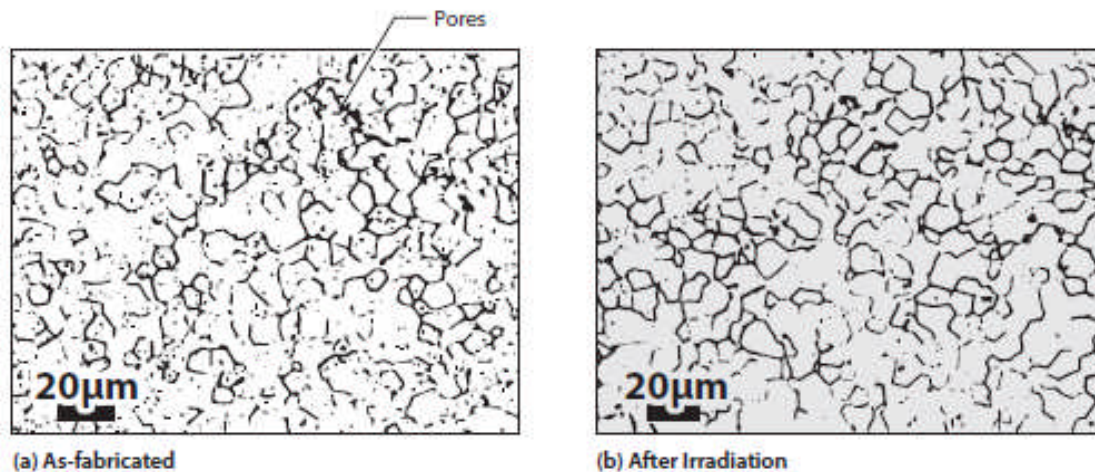
Note that the hoop stress is compressive in the inner part of the pellet and tensile in the outer part of the pellet. The tensile hoop stresses lead to radial cracking in the outer parts of the fuel pellet, as can be observed in Figure 15. The radial cracks add to the storage space for fission gas, reducing internal gas pressure. They also increase pellet expansion and hence sheath stress, encouraging detrimental environmentally assisted cracking (described in Section 8).

All three major components of stress are compressive in the central part of the pellet. This leads to compressive hydrostatic stresses, which reduce the size of fission gas bubbles at the grain boundaries. Moreover, the stresses are well into the plastic range. This can potentially lead to permanent deformations in the pellet. High local temperatures plus high local stresses can also lead to high rates of creep, leading to relatively rapid relaxation of stress. High local creep plus local plasticity are also believed to cause "dish filling" at high local temperatures.

7.2 Changes in Element Diameter and Length

During irradiation, several processes affect the diameter and length of the pellet and sheath. Notable among these are densification, swelling, creep, dish filling, thermal expansion, and hourglassing. Brief descriptions of these are given below.

Densification of pellets is caused primarily by irradiation-induced sintering of UO_2 in the reactor. Figure 17 shows an illustrative example of initial as-fabricated pores that have been removed during irradiation, resulting in densification. Although research has identified many factors that can affect densification, the relatively more important primary influences are believed to be temperature, initial density, and duration of high temperature.



[Source: Hastings, 1982]

Figure 17 Removal of as-fabricated pores during irradiation

Swelling of pellets is caused by fission products—solid as well as gaseous. The combined volume of solid fission products is larger than that of the parent material, resulting in swelling of the pellet. Unreleased fission gases also contribute to pellet swelling. For each percent atomic burnup, solid fission product swelling increases pellet volume by approximately 0.32% [Olander, 1976]. However, this number is subject to large uncertainties. [Note: 1 atomic percent = 240 MWh/kgU].

Creep due to external coolant pressure decreases sheath diameter. However, outward creep of the sheath can be expected if the internal gas pressure exceeds the coolant pressure.

Creep within the pellet is believed to cause axial expansion of the hot inner core of the pellet. This is also the region where dishes are located, as shown in Figure 1. In fuel that is operated at high local temperature, dishes are usually found to have become smaller after irradiation than before. This process is called dish filling.

The operating temperatures cause thermal expansion in the pellet as well as in the sheath. The pellet operates at much higher temperature than the sheath—for example, the average pellet temperature in the illustration in Figure 7 is about 1000°C, whereas the average illustrative sheath temperature in Table 1 is about 340°C. As well, the coefficient of thermal expansion of UO₂ is about twice that of Zr-4, as can be seen in Table 2. Therefore, the pellet usually expands much more than the sheath. At times, this results in the pellet filling the diametric gap and “pushing” the sheath outward. This in turn creates high tensile stresses in the sheath, often in the plastic range.

Diametric expansion of the pellet is usually much larger at the two ends of the pellet length than at the mid-point, as shown in Figure 18. This is called “hourglassing” and is caused by three factors: non-uniform temperature across the radius of the pellet, axial compression, and variations in initial density. These are illustrated in Figure 19 and explained below.

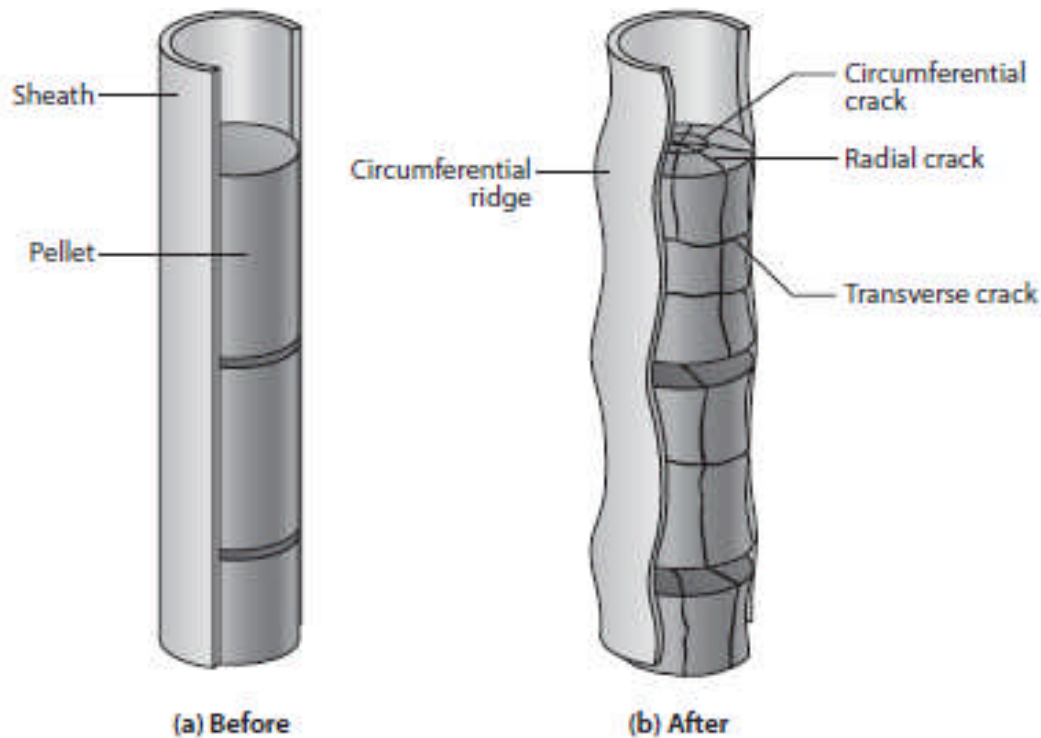
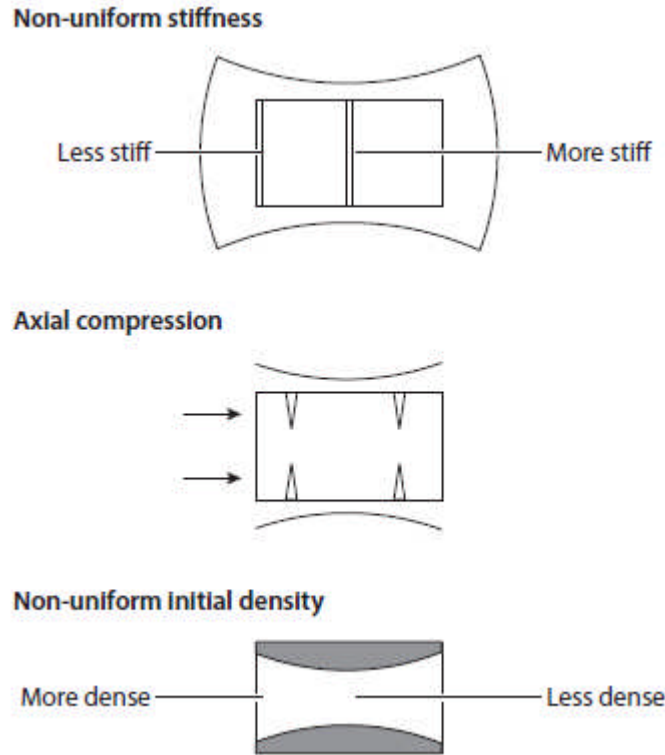


Figure 18 Fuel rod before and after startup

- **Non-uniform local stiffness:** As noted in Section 7.1, the parabolic temperature profile in the pellet leads to thermal stresses. The net diametric expansion of the pellet is influenced by these thermal stresses. However, these vary from one transverse cross section to the next. At the pellet mid-plane, the deformation of a transverse cross section is resisted, not only by the stiffness of that cross section, but also by the stiffness of the surrounding UO_2 . However, at and near the end of the pellet, a transverse cross section is surrounded by less UO_2 . Therefore, it can and does expand more than the cross section at the mid-plane of the pellet. This is one reason for pellet hourglassing.
- **Axial compression:** When the pellet expands axially, there may be axial interference between neighbouring pellets, between the stack of pellets and the endcap, or both. This results in compressive axial forces, which add to hourglassing. Axial compression has a larger influence on hourglassing if the force is applied near the surface of the pellet rather than near the centre.
- **Initial variation in pellet density:** One step during pellet fabrication is pressing of the pellet at its end (see Chapter 18). This causes the as-pressed densities to be higher near the end than at the centre. The pellet subsequently sinters during fabrication and during in-reactor densification. The resulting densification is higher at the mid-plane than at the ends because of the lower initial density at the mid-plane. This also contributes to hourglassing.



[Source: Tayal, 1987]

Figure 19 Causes of hourglassing in pellets

When an expanded hourglassed pellet pushes against the sheath, it causes “*circumferential ridges*” to be formed in the sheath at the ends of the pellets, giving the sheath the appearance that resembles a bamboo stalk, as shown in Figure 18. The circumferential ridges are locations of high stresses and strains, often well into the plastic range, and are a main location for environmentally assisted cracking, as discussed in the next section.

The pellet and sheath diameters change continually during irradiation in response to the processes described above and to continual changes in element power. This means that the pellet-to-sheath gap and the interface pressure between the pellet and the sheath also change continually during irradiation. These changes feed back to pellet temperature and to fission gas release, which in turn feed back to pellet expansion. Thus, a complex feedback loop is set up.

8 Environmentally Assisted Cracking

Environmentally assisted cracking (EAC) occurs in nuclear fuel when irradiation- and/or hydride-embrittled Zircaloy experiences high tensile stresses and strains in the presence of corrosive agents. These high stresses and strains are usually caused either by changes in power (called power ramps) or by excessive internal gas pressure. Figure 2 demonstrates that in the past, EAC caused by power ramps has been a dominant damage mechanism in CANDU fuels and suggests that CANDU fuels might have relatively low margins to defects from this mechanism.

Furthermore, our experience has been that when conditions are right for power-ramp EAC in a CANDU reactor, a number of fuel bundles tend to fail within a short period of time. As well, multiple fuel elements can often fail in a given fuel bundle. This combination can cause iodine

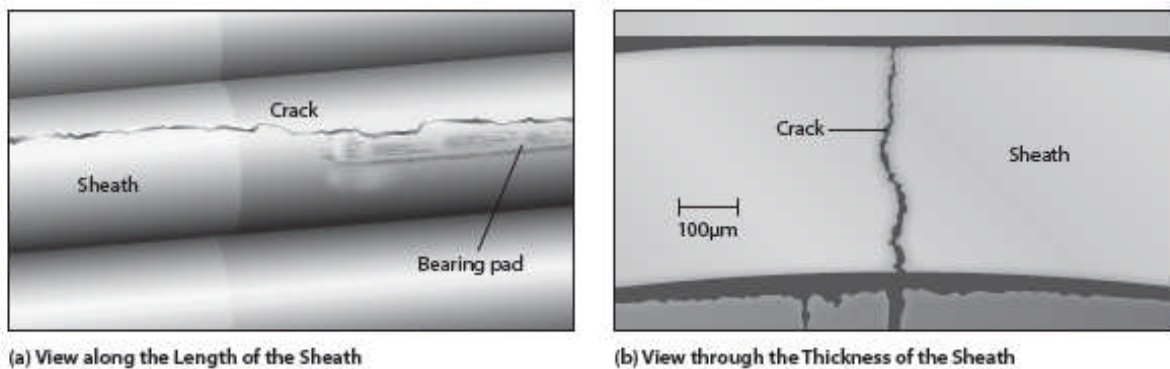
levels in the coolant to increase quickly. For the above reasons, it is particularly important to have a good understanding of this damage mechanism and of ways to quantify and control it.

To date, EAC has manifested in CANDU fuels through three main routes:

- EAC failures in the sheaths at interfaces between neighbouring pellets (called circumferential ridges) as a result of excessive pellet expansion during increases in power (called power ramps). Figure 20 shows an illustrative example [Penn *et al.*, 1977].
- EAC failures in sheaths near their welds with endcaps as a result of excessive pellet expansion during power ramps. Figure 21 shows an illustrative example of a typical crack near the sheath/endcap junction [Floyd *et al.*, 1992].
- EAC failures in the sheaths near their junctions with endcap welds as a result of excessive gas pressure accumulated during abnormally long residences of fuel in the reactor [Floyd *et al.*, 1992]. Such defects appear similar to those shown in Figure 21.

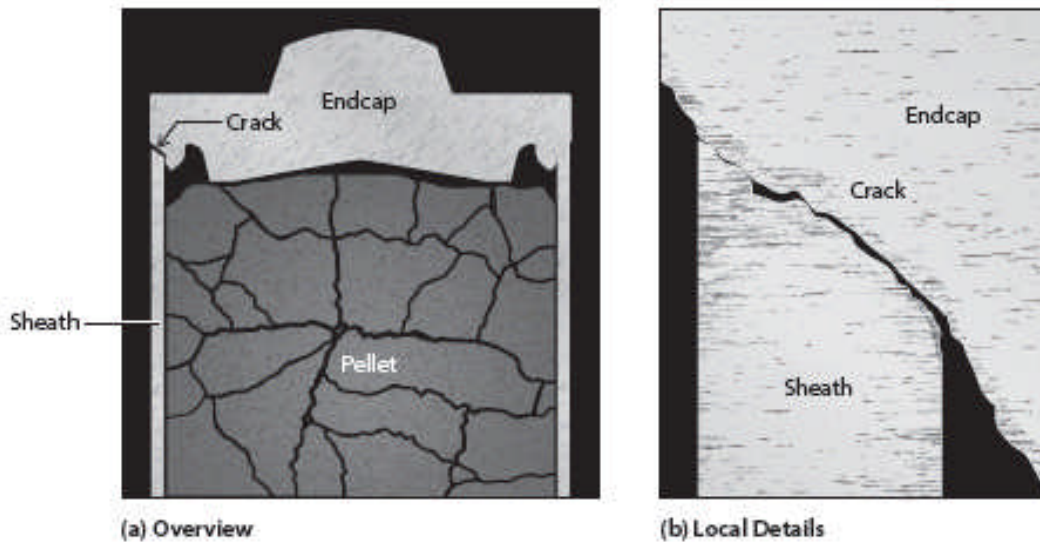
EAC is also called by other names in the scientific literature. In Canada, it is also called “stress corrosion cracking” (SCC). In the LWR community, it is usually called “pellet/clad interaction” (PCI). Both these names were coined shortly after the initial rash of power-ramp defects and were based on initial understanding of their mechanisms. Subsequently, much additional knowledge about the mechanism has been uncovered in a myriad of tests around the world. As a result, several labels very similar to EAC were proposed in later literature. In light of this additional information, a re-think in the early 2000s concluded that EAC is an appropriate label for this mechanism.

Figure 22 illustrates some key terms associated with EAC during power ramps.



[Courtesy COG]

Figure 20 Power ramp cracks originating at a circumferential ridge



[Courtesy COG]

Figure 21 Power ramp cracks near a sheath/endcap junction

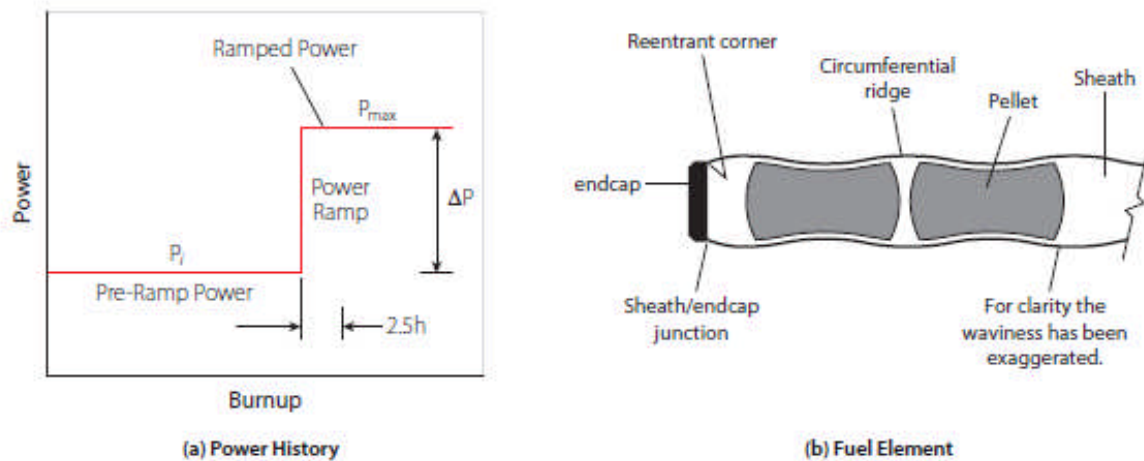


Figure 22 Key terms for environmentally assisted cracking during power ramps

8.1 EAC Processes

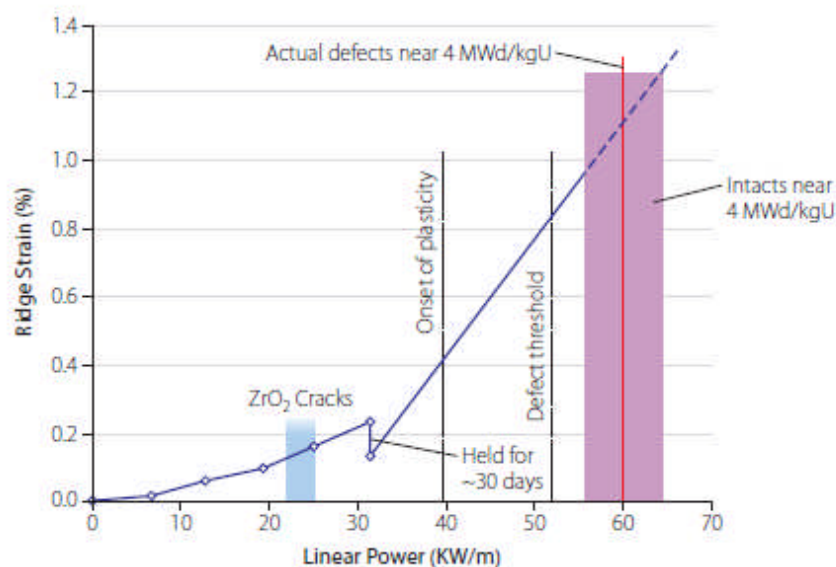
To control a CANDU reactor’s relative balances of neutronic powers in different parts of the reactor, CANDU fuel bundles can be repositioned in more than one axial location within a fuel channel. This is achieved by on-power refuelling, which is an important and unique feature of CANDU reactors.

Different parts of a fuel channel usually have different neutron fluxes, generally in a cosine

shape over the channel length. Therefore, during on-power refuelling, a previously irradiated fuel bundle can go from a relatively lower initial power to (or through) a relatively higher final or intermediate power. This causes power ramps in irradiated fuel elements.

The resultant pellet expansion strains and stresses the sheath, in the process breaking any protective layer of ZrO_2 that might have built up during initial irradiation. By then, the Zircaloy has also been embrittled by two processes: (a) by fast neutrons experienced during many months of irradiation at the low-power axial position, and (b) by hydrides, which can either promote or hinder initiation and growth of cracks depending on their orientation. In addition, by then, previous irradiation has also released fission products inside the fuel element, some of which are corrosive (such as iodine, cesium, and cadmium). Some fraction of these corrosive fission products is believed to react chemically with the CANLUB layer that is applied on the inside of the sheath, reducing the amount of fission products that are available to attack Zircaloy. The balance of the fission products is available for chemical attack on Zircaloy while the Zircaloy is also experiencing high stresses and strains due to the power ramp. These situations create a potentially potent combination for EAC: high stresses and strains, concurrent with embrittled Zircaloy, and also concurrent with a corrosive internal environment.

Figure 23 provides a specific example of some of the processes described above. It is based on in-reactor measurements of ridge strains during a power ramp to about 55 kW/m [Smith *et al.*, 1985]. Specifically, this fuel element was first irradiated in a base irradiation at about 30 kW/m to about 4 MW·d/kgU. Then it was inserted into an experimental rig that could measure sheath diameters during irradiation. The power in the experimental rig was first increased from 0 to about 30 kW/m, where it was held constant for about 30 days. Then the power was increased again, this time to about 55 kW/m.



[Source: Tayal *et al.*, 2008-2]

Figure 23 Mechanism for power ramp failures

On the plot in Figure 23 for ridge strain vs. element power, we have also superposed the strain at which ZrO_2 breaks and the strain at which Zr-4 becomes plastic [Tayal *et al.*, 2008-2]. One can see that ZrO_2 breaks very early during the ramp and therefore is unlikely to play a significant role in protecting the sheath from chemical attack by fission products. We can also see that defects start much later than when the sheath has become plastic. During the plastic part of loading, stresses increase but little, yet significant plasticity is required before EAC failures occur in CANDU fuel. Therefore, the primary mechanical driver of EAC is not stress alone, but rather a combination of stress and strain.

To maintain fuel integrity, the above combination needs to be managed to acceptable levels. This is done in part by designing and operating fuel below defect thresholds for EAC, as described in the next section.

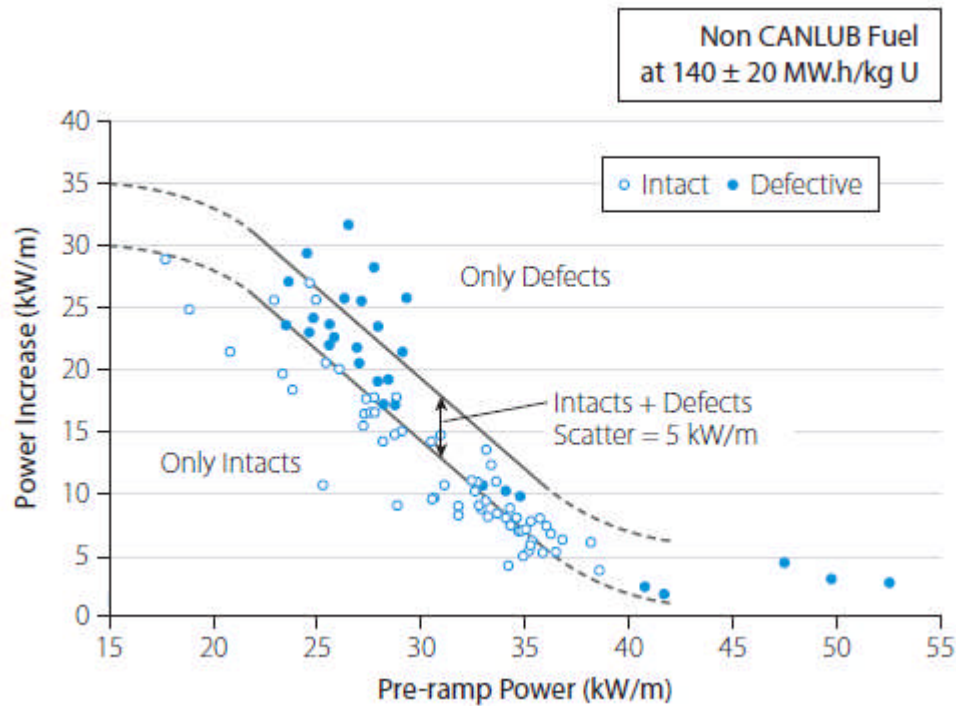
8.2 Defect Threshold

Like many processes, EAC contains some inherent variability. A defect threshold delineates an area below which no fuel defects are expected from EAC. Above the defect threshold, failures may or may not occur. Generally, the farther above a defect threshold the process is, the higher the probability of fuel defects.

An extensive literature of well over a thousand papers suggests that a very large number of parameters can potentially influence EAC. It is not practical to provide here an exhaustive mechanistic treatment of such a large list of parameters. Therefore, the authors have arbitrarily chosen to illustrate key concepts through a relatively recent insight [Tayal *et al.*, 2000]. It is acknowledged that other perspectives are also available in the literature, but they are not discussed here for reasons of space.

In the formulation described here, stresses and strains in Zircaloy are represented by the size of the power ramp (ΔP). Corrosive agent concentration is represented by a combination of pre-ramp power (P_i) and burnup (ω) at the time of the ramp. Material degradation is represented by the burnup at the time of the ramp (ω).

Figure 24 shows the empirically obtained defect threshold at 140 ± 20 MWh/kgU for non-CANLUB fuel.



[Source: Tayal *et al.*, 2000]

Figure 24 Defect threshold due to power ramp in non-CANLUB fuel at 140±20 MWh/kgU

The figure contains two lines. The lower line is the defect threshold for non-CANLUB fuel. Based on empirically derived curves, the defect threshold for CANLUB fuel is located about 12 kW/m higher than that shown in Figure 24 [Tayal *et al.*, 2000].

Exercises:

Consider a non-CANLUB fuel element for which the operator is contemplating a power ramp from 30 kW/m to 50 kW/m for 2 hours at 140 MWh/kgU. Its pre-ramp power, P_i , is 30 kW/m. Its power ramp, ΔP , is $(50 - 30) = 20$ kW/m. From Figure 24, the fuel element can withstand a power ramp of about 14 kW/m at 140 MWh/kgU. Therefore, the applied power ramp will exceed the defect threshold and expose the fuel element to risk of an EAC defect.

As a second exercise, consider the same ramp being applied to a CANLUB fuel element. Its defect threshold is at $(14 + 12) = 26$ kW/m. The applied ramp of 20 kW/m is less than its defect threshold, and therefore the fuel can be expected to survive the ramp.

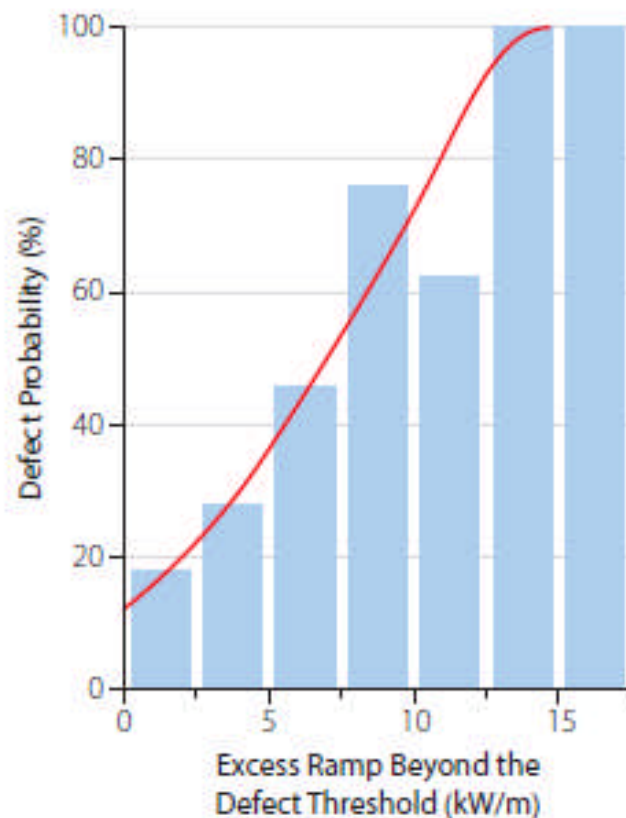
8.3 Defect Probability

The basic rule is always to operate fuel in a region which is safe from EAC defects, i.e., below the defect threshold. Nevertheless, on very rare occasions it may become necessary to operate a small number of fuel bundles slightly above the defect threshold in a one-off situation that might have become unavoidable due to an unusual combination of circumstances, such as during restart under a distorted flux shape after a shutdown. One then needs to consider taking a calculated risk. To develop an effective strategy for such rare occasions, one needs to quantify the risk of fuel failure above the defect threshold. This is done through knowledge of defect probability beyond the defect threshold, as described below.

Figure 24 contains not one, but two lines. As noted earlier, the lower line is called the defect threshold; it is the line below which no defect occurs. The upper line is one above which no fuel bundle stays intact. The region in between contains some scatter: some bundles in that region fail, whereas others stay intact.

Empirical evidence suggests that for all practical purposes, the defect threshold represents a trivial likelihood of defect, essentially zero. Nevertheless, in statistical theory, probabilities usually have asymptotic ends, that is, a probability is never zero, nor is it ever 100%. Therefore, the defect threshold shown in Figure 24 is usually assigned a low arbitrary probability such as 1%. Likewise, the upper line in Figure 24 is usually assigned an arbitrarily high defect probability close to 100%.

Figure 25 shows an illustrative increase in defect probability as a fuel bundle experiences power ramps that exceed the defect threshold [Penn *et al.*, 1977]. Theoretically, the probability should be an “S”-shaped curve with asymptotic ends. For practical purposes, however, empirical evidence shows that the asymptotic parts near the two ends are small and that for the most part, the defect probability increases essentially linearly with increasing distance from the defect threshold (see Figure 25).



[Source: Penn *et al.*, 1977]

Figure 25 Defect probability

The distance between the two lines shown in Figure 24 is about 5 kW/m; however, when the data from other burnups are also considered, the overall separation between the two lines for all burnups is closer to 10 kW/m. Therefore, to a first approximation, and if one ignores small asymptotic regions near the two extremes, for every increment of one kW/m above the defect threshold, the defect probability increases by about 10 percentage points until it reaches 100%.

The portion of the ramp that is above the defect threshold is sometimes also called the “excess ramp”. In the illustrative example below, the “excess ramp” is 8 kW/m.

Exercise: Consider a non-CANLUB fuel bundle where the steady-state power in the outer element changes from 35 kW/m to 50 kW/m at 140 MWh/kgU. This gives it a ramp of $(50 - 35) = 15$ kW/m. From Figure 24, the defect threshold at this initial power is 7 kW/m. Therefore, the actual ramp is $(15 - 7) = 8$ kW/m above the defect threshold. Therefore, this fuel bundle has a $(8 * 10\%) = 80\%$ chance of fuel defects through EAC.

8.4 Mitigation

Based on past experience, the fuel industry has adopted certain strategies to mitigate EAC defects. Some illustrative examples are given below.

- **CANLUB:** CANLUB significantly increases the defect threshold. It is believed that the effectiveness of CANLUB increases with thickness. However, it is also believed that after a certain thickness, additional increases in CANLUB thickness likely yield diminishing returns. At the same time, there is concern that very thick layers of CANLUB may potentially release excessive hydrogen into the sheath. Therefore, a CANLUB layer of a selected optimal thickness is applied to the inside of the sheath [Wood and Hardy, 1979].
- **Fuel Management:** The key operating parameters for EAC—size of the power ramp, initial and final powers, and burnup—are all controllable to some degree through refuelling strategy. Therefore, optimal refuelling strategies have been devised to avoid EAC failures in CANDU reactors. A compelling example comes from the Pickering reactors, where early EAC failures were eliminated in part by improved refuelling schemes.
- **Sheath/Endcap Junction:** A significant contribution to EAC defects at sheath/endcap junctions arises from the stress concentration at re-entrant corners of these junctions. Therefore, the detailed design of the sheath/endcap junction must be carefully controlled, including the radius of the re-entrant corner, the pellet profile at the end of the fuel stack, and the axial distance between the pellet stack and the re-entrant corner.
- **Element Rating:** Smaller ramps and lower heat generation rates reduce the threat from EAC, as shown in Figure 24. These can be achieved by, for example, spreading a bundle’s power among more fuel elements, e.g., by using more but smaller-diameter fuel elements within a fuel bundle. CANDU fuel has indeed evolved in this direction, starting with a fuel bundle that used 19 fuel elements, then moving to one that used 28, to 37 elements, and to the CANFLEX design that uses 43 fuel elements [Hastings *et al.*, 1989].
- **Detailed Internal Design:** Sheath strain and fission gas release can also be influenced by the detailed internal design of the fuel element, such as pellet density and clearances between the sheath and the pellets.

9 Vibration and Fatigue

Fuel elements produce large amounts of heat and therefore must be cooled aggressively. Coolant velocity is usually high (about 10 m/s), and the flow is at least partly turbulent. Moreover, the coolant may sometimes contain standing waves of pressure pulses. The pressure pulses are created when a pump's vanes pass over the pump outlet and may be subsequently amplified by resonance in pipes that carry the coolant. These combinations of conditions can lead to vibrations and rocking in fuel elements and bundles and even in fuel strings. This in turn creates the potential for fatigue and fretting.

In a significant defect excursion, these conditions did indeed occur in 1991 in the Darlington reactors in Canada. This led to excessive axial vibrations in the fuel strings, which cracked endplates in fatigue and also caused significant fretting of spacer pads [Lau *et al.*, 1992]. This in turn led to shutdown of the reactors for a few months and significant loss of revenue.

To avoid damage due to fatigue and fretting, one needs to understand the science behind fuel vibrations and the resulting alternating stresses and incorporate appropriate mitigation strategies in the design and operation of the fuel and the plant. The next section describes some aspects of the science of fuel vibration and fatigue.

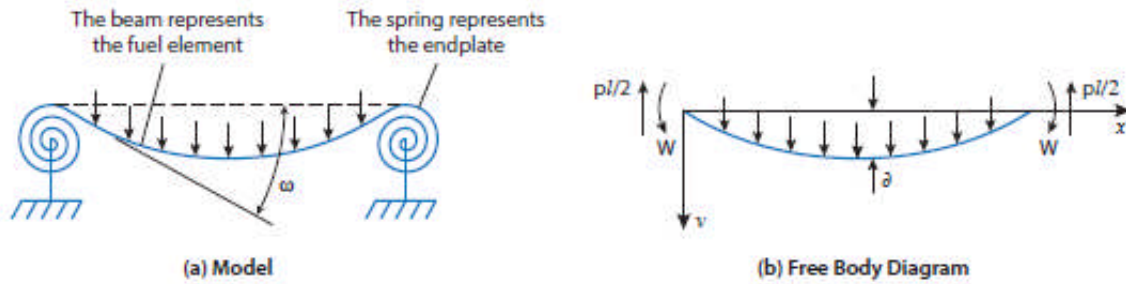
9.1 Alternating Stresses

Axial flow and turbulence induce lateral vibrations in fuel elements, whereas pressure pulses induce axial vibrations. Both types of vibrations generate alternating stresses in the fuel bundle endplate and in the assembly weld (that is, the weld between the endplate and the endcap).

Quantification of alternating stresses and the resulting fatigue due to lateral vibrations involves a number of calculations, such as the bending moment in the assembly weld and in the endplate due to bending of a fuel element, the resulting alternating stresses, and a comparison of these stresses to the fatigue strengths. Mathematical models to do this are available [Tayal *et al.*, 1984] and are summarized below.

9.1.1 Moment Due to Fuel Element Deflection

The overall model is shown in Figure 26. If a fuel element of length ℓ experiences a uniformly distributed load p that deflects it in a direction radial to the fuel bundle, its lateral deflection v is resisted by its own moment of inertia as well as by the stiffness of the two endplates. The endplates are twisted by the fuel element and therefore act as torsional springs in resisting the twisting moment W applied by the fuel element.



[Source: Tayal *et al.*, 1984]

Figure 26 Lateral vibration of a fuel element

If the fuel element's flexural rigidity is J , the classical equation for beam deflection v can be written as [Gere *et al.*, 1997]:

$$J \frac{d^2v}{dx^2} = W - px(\ell - x)/2, \quad (6)$$

where x represents the distance along the length of the fuel element.

For boundary conditions of:

$$v = 0 \text{ at } x = 0 \text{ and at } x = \ell, \quad (7)$$

Equation (6) integrates to:

$$Jv = Wx(x - \ell)/2 + px(x^3 - 2x^2\ell + \ell^3)/24. \quad (8)$$

To derive an expression for the moment transmitted through the assembly weld, consider the relationship between the moment and rotation of the spring:

$$\frac{dv}{dx} = \omega = W/S \text{ at } x = 0, \quad (9)$$

where ω represents the rotation of the fuel element.

By differentiating Equation (8) to obtain the fuel element's slope at the end and inserting this into Equation (9), we obtain a relationship for the moment W transmitted by the fuel element to the endplate through the assembly weld [Tayal *et al.*, 1984]:

$$W = \frac{p\ell^2}{12} \left[\frac{1}{1 + \frac{2J}{S\ell}} \right]. \quad (10)$$

Equation (10) expresses the moment carried by the endplate and the assembly weld in terms of

the uniformly distributed load p . However, p is usually not known. Instead, the mid-span deflection δ can be estimated more easily through other means. Therefore, p can be replaced in Equation (10) by the mid-span deflection δ using the following additional information:

$$\delta = v \text{ at } x = \ell/2. \quad (11)$$

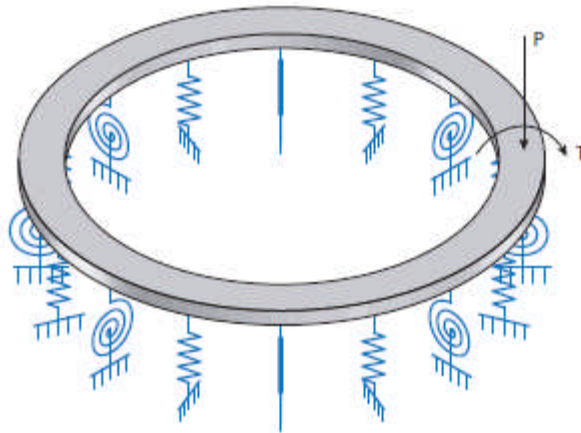
This results in the following equation for the moment carried by the assembly weld and the endplate as a function of the mid-length deflection of the fuel element:

$$W = 32J\delta/(\ell^2 + 10J\ell/S). \quad (12)$$

To calculate the moment through the above equation, one needs to know the spring constant S of the endplate, which is discussed in the next subsection.

9.1.2 Spring Constant of the Endplate

The moment W as calculated above twists the endplate by a force which decays along the circumference of the endplate. As the endplate twists, it forces its own local twist on the fuel elements that are welded to it, which the latter resist. Therefore, the applied twisting moment on the endplate is resisted not only by the torsional rigidity of the endplate, but also by the torsional rigidities of the other fuel elements welded to the endplate. For this reason, the endplate behaves like a beam resting on an elastic foundation. Figure 27 shows such a model.



[Source: Tayal *et al.*, 1984]

Figure 27 Endplate as a beam on elastic foundations

The endplate rings are circular. Sensitivity studies show that under on-power conditions of CANDU fuel elements, the effect of circularity is small. Therefore, to a good first approximation, the mathematics of the endplate can be simplified considerably by treating it as a straight (rather than circular) beam on elastic foundations. A mathematical model for this can be developed based on the science given in classical textbooks on mechanics of materials [for example, see Timoshenko, 1961].

Let β be the local twist of the beam. A foundation of modulus κ will exert a twisting moment of $-\kappa\beta$ per unit length of the beam. If the beam's cross section is assumed to carry only a twisting

moment M_z , then the equilibrium of an infinitesimal length yields:

$$\frac{dM_z}{dz} = GC \left(\frac{d^2 \beta}{dz^2} \right) = \kappa \beta, \quad (13)$$

where z is the distance along the length of the beam, G is the shear modulus, and C is the twisting moment of inertia.

This second-order differential equation can be integrated to yield the rotation and the twisting moment along the beam's length. The two constants of integration can be obtained by the requirement that the rotation be zero at infinite distance from the origin and that the internal twisting moment at the origin be half the applied twist. This process yields the following equations:

$$\beta = \frac{T\alpha}{2\kappa} e^{-\alpha z}, \quad (14)$$

where T is the applied twisting moment and

$$\alpha = \{\kappa/(GC)\}^{1/2}. \quad (15)$$

If the beam's response to W is represented as a torsional spring, its spring constant S is:

$$S = \left. \frac{T}{\beta} \right|_{z=0} = 2(GC\kappa)^{1/2}. \quad (16)$$

The above spring constant can be used in Equation (12) to calculate the moment carried by the assembly weld.

9.1.3 Foundation Modulus

Equation (16) requires knowledge of the foundation modulus κ for the endplate.

Let two endplate rings of radius R connected by N fuel elements be twisted by an angle β . The ends of each sheath, which are held perpendicular to the endplate surface by the assembly weld, will also rotate by the same angle β . If W represents the resistive moment applied by each sheath to the endplate, then m , the resistive moment from the sheath per unit endplate length, can be evaluated by spreading the total of such moments over the circumference of the endplate:

$$m = NW/(2\pi R). \quad (17)$$

W is also equal to the bending moment applied by the endplate to the fuel element to rotate its end by β . Therefore, classical beam theory can be used to relate W and β as follows:

$$\beta = W\ell/(2J). \quad (18)$$

Therefore, by combining Equations (17) and (18), the foundation modulus κ can be calculated as:

$$\kappa = m/\beta = JN/(\pi R\ell). \quad (19)$$

To account for the tight contact with the neighbouring fuel bundle under high hydraulic load, it is customary to assume twice the actual number of fuel elements in Equation 19 above.

9.1.4 Cross-Sectional Properties of the Endplate

The equations presented above also require knowledge of the endplate's twisting moment of inertia (C) and the fuel element's flexural rigidity (J).

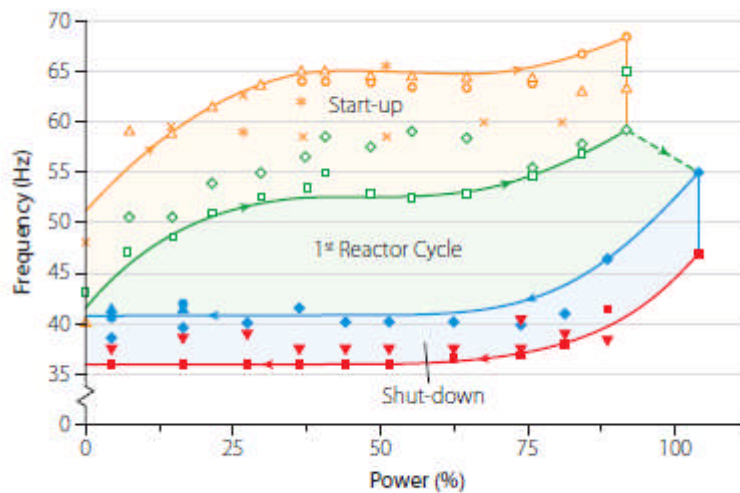
The twisting moment of inertia C of the endplate can be obtained from the classical equation for a rectangular beam. For the usual shapes of CANDU endplates [Tayal *et al.*, 1984]:

$$C = 0.26ct^3, \quad (20)$$

where c is the width of the beam and t its thickness.

9.1.5 Flexural Rigidity of the Fuel Element

At high power, the pellet expands and grips the sheath tightly, often stretching the latter well into the plastic range. Therefore, the flexural rigidity of a fuel element usually contains contributions from the sheath and from the pellets. The concept can be illustrated more simply by examining the experimental results shown in Figure 28.



[Source: Pettigrew, 1993]

Figure 28 Stiffening of a fuel element at operating power

When the instrumented fuel element represented in Figure 28 was initially brought to high power, its vibration frequency increased significantly [Pettigrew, 1993]. Frequency of vibration can be related to flexural rigidity through the classical theory of vibration. This suggests that at initial high power, the flexural rigidity of the fuel element is significantly higher than that of an empty sheath. The difference reflects the contribution of the pellet when it is in tight contact with the sheath.

However, the pellet is not always in tight contact with the sheath. With continued irradiation, the interfacial pressure between the pellet and the sheath relaxes due to creep. This in turn lowers the net flexural rigidity of the fuel element and hence decreases its vibration frequency. Lower power also reduces the pellet/sheath interfacial pressure. These dynamics are also reflected in Figure 28. For this reason, we express the flexural rigidity of the fuel element as

that of the sheath plus that of the pellet multiplied by a “pellet interaction factor” G which reflects the varying levels of pellet/sheath interaction.

Another complication is that UO_2 is brittle and therefore cannot support significant tensile loads. Therefore, the resulting equation for pellet flexural rigidity is fairly complex, as described for example in [Tayal *et al.*, 1984]. For simplicity, here we treat the impact of pellet cracking by means of a pellet cracking factor α which reduces the net contribution of the pellet to the overall flexural rigidity of the fuel element. As an illustrative number, the examples below use a pellet cracking factor α of 0.1.

Therefore, the net flexural rigidity J of the fuel element can be described as:

$$\begin{aligned} J &= J_s + GJ_p \\ &= E_s \left[\frac{\pi}{4} (r_1^4 - r_2^4) \right] + \frac{\pi}{4} E_p r_p^4 \alpha G \end{aligned} \quad (21)$$

where J is the flexural rigidity of the fuel element, J_s the flexural rigidity of the sheath, J_p the flexural rigidity of the pellet, E_s the Young’s modulus of the sheath, r_1 the outer sheath radius, r_2 the inner sheath radius, E_p the Young’s modulus of the pellet, r_p the pellet radius, α the pellet cracking factor, and G the pellet interaction factor.

The pellet interaction factor G varies between 0 and 1. Under the conditions of the experiment shown in Figure 28, the pellet interaction factor G is zero when the fuel element is at zero power. When the fuel element is first brought to full power, G increases to 1 because the interfacial pressure between the pellet and the sheath is high. During continued operation at full power, G gradually decreases to 0 as the interfacial pressure between the pellet and the sheath relaxes. Therefore, the pellet/sheath interfacial pressure has a major impact on the pellet interaction factor.

For a given lateral deflection of the fuel element, stresses in the endplate and in the assembly weld are higher for higher levels of pellet/sheath interaction. Therefore, the upper end of the pellet interaction factor range gives conservative results for such stresses.

9.1.6 Stresses

The above Equations (12), (16), (19)–(21) provide all the information needed to calculate the moment carried by the assembly weld and the endplate. This moment can be converted into nominal stresses using the classical equations given below [Timoshenko *et al.*, 1970].

Nominal shear stress τ in the endplate:

$$\tau = 1.87 W / (ct^2). \quad (22)$$

Nominal normal stress σ in the assembly weld:

$$\sigma = 32 W / (\pi d^3), \quad (23)$$

where d is the weld diameter.

To the nominal stresses given by the above equations, one would need to add the effects of stress concentrations due to the rapid change in geometry near the end of the fuel element. This topic is covered as part of fatigue strength in Section 9.2.

9.1.7 Illustrative Example

As an illustrative example, let us calculate the nominal stresses in the endplate and in the assembly weld when the outer fuel element of a CANDU-6 bundle undergoes lateral vibrations 25 micrometers in amplitude.

Assume that the fuel dimensions and properties are as given in Tables 1 and 2, except that the on-power diametric clearance between the pellet and the sheath is zero. For the remaining inputs, assume that the mean radius R of the endplate's outer ring is 43 mm, the weld diameter d is 4 mm, the pellet cracking factor α is 0.1, and the rigidity enhancement factor G is 1.

Equations (20), (21), (19), (16), and (12) yield the following intermediate results: the twisting moment of inertia C of the endplate is 5.2 mm^4 , the flexural rigidity J of the fuel element is 46 Nm^2 , the foundation modulus κ of the endplate is $25 \text{ kNm}/(\text{m}\cdot\text{rad})$, the spring constant S is $118 \text{ Nm}/\text{rad}$, and the bending moment W is 0.017 Nm .

Equation (22) gives the nominal shear stress in the endplate as 2.5 MPa. Equation (23) gives the nominal normal stress in the assembly weld as 2.7 MPa.

Because these stresses are due to vibration, they are alternating stresses. Their impacts on fatigue are examined in the next section.

9.2 Fatigue of the Endplate and the Assembly Weld

O'Donnell and Langer recommended 55 MPa as the endurance limit for cold-worked and/or welded Zircaloy-4 at 300°C [see O'Donnell *et al.*, 1964]. This assumes that residual stresses are equal to cyclic yield strength, accounts for damage due to irradiation, and includes a safety factor of two to cover miscellaneous effects such as specimen size, environment, surface finish, and data scatter.

The diameter of the fuel element endcap decreases sharply near the weld. Hence, stress concentrations are to be expected in this region. Therefore, the endurance limit specified above should be reduced by the effects of stress concentration. Peterson's ∂ concept can be used for this purpose [see Peterson, 1943]. It states that in a region of sharp stress concentrations, fatigue is best evaluated through stress at a distance ∂ below the surface. ∂ is a material property.

Based on experimental data, O'Donnell and Langer estimated $\partial=50$ micrometers for Zircaloy-4. Fatigue strength reduction for this delta can be determined using the results of O'Donnell and Purdy [see O'Donnell *et al.*, 1963]. A review of O'Donnell and Purdy's results shows that for a fairly wide range of notch radii (30 to 200 micrometers), the fatigue strength reduction factor K is between 2.0 and 2.5 when the section width is 5 mm (close to the CANDU assembly weld). For purposes of illustration, let us conservatively assume a fatigue strength reduction factor K of 2.5 for the assembly weld (i.e., the weld between the endcap and the endplate).

There are no major geometric stress raisers in an endplate that would bear significantly on fatigue due to alternating shear stress near the assembly weld. Nevertheless, a small undetected fabrication flaw (e.g., a crack) will act as a notch and reduce local fatigue strength. Such a small crack may exist due to a flaw in the sheet metal used for endplate fabrication or may be introduced during bundle assembly and subsequent handling. Using the curves of O'Donnell and Purdy, the fatigue strength reduction factor for an endplate in the presence of such a small crack can be conservatively estimated as 2. Therefore, the fatigue strength of the endplate is 28

MPa.

Exercise:

Consider the potential of fatigue from lateral vibrations of the fuel element assessed in Section 9.1.6.

Assembly weld: The alternating stress is 2 MPa. The fatigue strength is 22 MPa.

Endplate: For comparison to fatigue strength, the classical von Mises formulation for effective stress tells us that shear stress needs to be multiplied by the square root of 3 to be comparable to normal stress. Therefore, the effective alternating stress in the endplate is $(2.5 * \sqrt{3}) = 4.4$ MPa. In comparison, the fatigue strength is 28 MPa.

For both the assembly weld and the endplate, the alternating stresses are much lower than the corresponding fatigue strengths. Therefore, the weld and the endplate are not at risk of fatigue failures from this level of vibration.

10 Fuel Design Verification

During design, fabrication, and operation of nuclear fuel, a key objective is to preclude, as a minimum, significant, chronic, systematic fuel failures. This needs to be confirmed up front for credible combinations of the most demanding design, fabrication, and operating conditions that can be expected in the reactor.

During design, likelihood of acceptable fuel performance can be assessed through a mixture of three types of tools: engineering judgment, tests, and analyzes. Each tool has its pros and cons, as explained later in this section, and therefore judicious combinations of them tailored to each specific situation are often used.

Tests can be done on prototype fuels either inside or outside a reactor. In-reactor tests can be done either in a test reactor such as the NRU and NRX reactors in Chalk River, Ontario, or in an operating commercial power reactor. In-reactor tests automatically include the effect of neutrons, which out-of-reactor tests miss. However, out-of-reactor tests can include certain influences that are not available in current in-reactor experimental facilities, such as the effect of gravity (current test loops are vertical) and the effect of the precise support provided to the fuel string by shield plugs, sidestops, or latches (in current test loops, fuel is supported by a central structural tube). In addition, out-of-reactor tests often tend to be significantly less expensive and quicker than in-reactor tests. Judicious choices must therefore be made in each situation.

Tests have a significant advantage over analyzes in that they automatically include all processes encompassed by the test conditions. Therefore, within the parameters of the experiment, there is virtually no risk that an important process has been missed. Table 3 is an illustrative list of tests done on some CANDU prototype fuels.

Table 3 Illustrative list of tests on prototype fuel bundles

Test	Purpose and Configuration
Bent-tube passage	Bench test done at room temperature and atmospheric pressure to verify that a prototype bundle, when not damaged, can pass through the “bent-tube” gauge, which simulates the most restrictive passage in a fuel channel.
Bundle strength – shield plug support	Single-bundle test done in stagnant water at reactor pressure and temperature to verify that a prototype bundle, supported by a simulated shield plug, can withstand the maximum reactor load in the fuel channel under normal conditions without failing. Test bundle failure is indicated when: (1) the bundle fails the bent-tube gauge test and/or (2) shows permanent deformation in any of its components that exceeds the as-built dimensional tolerances for that component and/or (3) develops cracks in any of its structural components or joints between components.
Bundle strength – double side stop support	Single-bundle test done in stagnant water at reactor pressure and temperature to verify that a prototype bundle, supported (normally) by two side stops, can withstand the maximum reactor load in the fuel channel during refuelling without failing. Test bundle failure is indicated when: (1) the bundle fails the bent-tube gauge test and/or (2) shows permanent deformation in any of its components that exceeds the as-built dimensional tolerances for that component and/or (3) develops cracks in any of its structural components or joints between components. Applies to C6-type reactors.
Bundle strength – single side stop support	Single-bundle test done in stagnant water at reactor pressure and temperature to verify that a prototype bundle, supported (abnormally) by a single side stop, can withstand the maximum reactor load in the fuel channel during refuelling without failing. Test bundle failure is indicated when the bundle fails the bent-tube gauge test. Applies to C6-type reactors.
Refuelling Impact	Out-of-reactor test done in a representative full-length fuel channel using circulating light water at reactor operating temperature and pressure, to verify that prototype bundles can withstand the maximum impact loads expected in the fuel channel during refuelling without failing. Test bundle failure is indicated: (1) when the bundle fails the bent-tube gauge test and/or (2) shows permanent deformation in any of its components that exceeds the as-built dimensional tolerances for that component and/or (3) develops cracks in any of its structural components or joints between components. Applies to C6-type reactors.

Test	Purpose and Configuration
Endurance	Out-of-reactor test, done inside a representative full-length fuel channel containing a full complement of prototype fuel bundles, using circulating light water at reactor operating temperature and pressure, in increments of time until the spacer pads of the test bundles cease to exhibit additional wear with increases in test time, to verify: (1) that spacer pad wear on test bundles does not exceed its wear allowance; (2) that bearing pad wear on test bundles, projected over the maximum in-reactor bundle residence time, does not exceed its wear allowance; (3) that test bundles do not show permanent deformation in any of their components that exceeds the as-built dimensional tolerances for those components; (4) that test bundles do not develop cracks in any of their structural components or joints between components; and (5) test bundles do not cause channel damage, projected over the lifetime of the channel, which exceeds the channel's lifetime material loss allowance, also taking into account possible channel damage by other means.
Sliding wear	Single prototype bundle test done in stagnant light water at reactor operating temperature and pressure to verify that: (1) bearing pad wear in the test bundle does not exceed the bearing pad wear allowance and (2) projected lifetime pressure-tube damage, caused by sliding bearing pads of the test bundle, does not exceed the channel's lifetime material loss allowance, also taking into account possible channel damage by other means.
Pressure drop	Out-of-reactor test done in a representative full-length fuel channel, containing a full complement of prototype fuel bundles, using circulating light water at reactor operating temperature and pressure, to verify that the hydraulic pressure drop generated in the portion of the fuel channel that contains fuel bundles does not exceed the pressure drop allowance for the same portion of the channel.
Bundle rotation pressure drop	Out-of-reactor test done in a representative full-length fuel channel and/or a partial-length channel, using circulating light water at reactor operating temperature and pressure and/or at room temperature and low pressure, to determine the variation in hydraulic pressure drop generated across the endplate-to-endplate junction between two abutting prototype bundles as a function of their relative radial (mis)alignment.
Fuelling machine compatibility	Out-of-reactor test done in a representative full-length fuel channel, using circulating light water at reactor operating temperature and pressure, in conjunction with a production fuelling machine, to verify that the fuelling machine can charge and discharge prototype fuel bundles into the channel.
Wash-out	Out-of-reactor test done in a representative full-length (or partial-length)

Test	Purpose and Configuration
	fuel channel, using circulating light water at reactor operating temperature and pressure, in conjunction with apparatus that simulates the relevant functions of the fuelling machine, to determine what malfunctions in use of carrier tubes might cause “wash-out” of the type observed in some power reactors. Applies to CANDU reactors that use carrier tubes during refuelling.
Frequency sweep	Out-of-reactor test done in a representative full-length fuel channel containing a full complement of prototype fuel bundles, using circulating light water at reactor operating temperature and pressure and a pressure pulse generator, to: (1) determine the frequency of pressure pulsations at which the column of test bundles, supported normally inside the channel, may resonate, and (2) verify that the resonant frequency of the column of test bundles is not the same (or nearly the same) as the coolant pump vane passing frequency.
Critical heat flux	Out-of-reactor test done in a representative full-length fuel channel using circulating light water at reactor operating temperature and pressure and electrical heaters to simulate the geometry and power produced by fuel bundles, to determine the spectrum of channel thermal-hydraulic and power conditions in the range of interest to reactor operation, which lead to a step change in heater surface temperature, referred to as “dryout”.
High-power irradiation	Irradiation test done on prototype bundles cooled by circulating water at reactor operating temperature and pressure to verify that a bundle irradiated at power/burnup conditions that encompass the power/burnup conditions of all bundles in the power reactor will be defect-free at the end of the irradiation period. Such a test can be done, for example, in a vertical channel of the NRU test reactor, called a “hot loop”, in which test bundles are cooled by light water; enriched uranium would need to be used to generate the high element ratings expected in a commercial CANDU power reactor.
Power ramp irradiation	Irradiation test done on prototype bundles cooled by circulating water at reactor operating temperature and pressure, to verify that a test bundle can survive, defect-free, the most severe power ramps expected in a reactor. Typically, this would involve: (1) irradiation of a test bundle at relatively low power for some fraction of its residence in the reactor, and then (2) an increase in power for the remainder of its residence in the reactor, such that the burnup accumulated at the initial power and the increased power surpasses the equivalent conditions of all bundles in the power reactor. Using C6 as an illustrative example, the low-power irradiation would reflect power and burnup in positions 1 to 4 in a high-power channel, and the size of the ramp would reflect, in an appropriately conservative manner, the power ramps in bundles 1 to 4 during or after

Test	Purpose and Configuration
Irradiation of special materials	<p>their shift to positions 9 to 12. Such tests can be performed in, for example, the vertical hot loops at NRU in CRL in which test bundles are cooled by light water; enriched uranium pellets would be required to achieve the high element powers expected in a commercial CANDU reactor.</p> <p>Irradiation test done on prototype elements which contain the novel material (e.g., an inert matrix for burning of actinides) cooled by circulating water at reactor operating temperature and pressure, to verify that the elements containing the special material will be defect-free at the end of their irradiation period. Such a test can be done, for example, in “de-mountable” bundles in a vertical channel of the NRU test reactor called a “hot loop”, in which test specimens are cooled by light water.</p>

At the same time, fully representative tests are not always practical in some situations, for example because of equipment, cost, schedule, or combinations thereof. As specific illustrative examples, let us consider the following:

- Comprehensiveness:** As one illustrative example, a CANDU fuel designer needs to confirm, among other aspects, that a fuel bundle has adequate mechanical strength to resist the mechanical loads imposed on it during discharge from the fuel channel. The test facility, to verify this experimentally, would need to provide for all the important effects in this scenario, meaning that (a) the test facility should be shielded so that it can accommodate irradiated fuel so that reduction in ductility due to prior irradiation can be accounted for; (b) it should be long enough to accommodate a string of approximately 12 fuel bundles; (c) it should produce power to simulate the effect of on-power interaction of the pellets and the sheath on load shedding; (d) it should be connected to a pump of sufficiently large capacity to provide the necessary flow for the hydraulic drag load; and (e) it should contain a representative fuel support configuration to simulate the appropriate load concentrations. We currently do not have a shielded facility that meets all these requirements, and building a new one would be very expensive and time-consuming. For this reason, such tests have been done in the past in unshielded out-of-reactor facilities using non-irradiated fuel bundles. Although such tests are useful, they do miss the order-of-magnitude drop in ductility of the fuel bundle’s structural materials that occurs during irradiation, and hence they may not always determine the actual adequacy of an irradiated fuel bundle’s mechanical strength. Another similar situation that is also not covered by existing test facilities is the effect of gravity on long-term irradiation-enhanced creep sag of fuel in a horizontal orientation. These situations can be rectified through analyzes.
- Scatter:** As another illustrative example, consider the need to verify whether or not a new fuel design meets the expected power ramp challenges in a new operating envelope for which the EAC defect threshold is not well known ahead of time (*a priori*). For a new operating envelope and fuel design, one would not know *a priori* which specific ramp is the most demanding. Therefore, one would need to test many ramps, and to cover the expected scatter in the results, one would need to test a statistically significant number for each condition. This would require testing many bundles for a large number

of ramps, and for each ramp, significant in-reactor irradiation would be required to accumulate the required burnup. Because only limited facilities for in-reactor irradiation are available, the full test matrix could require large amounts of time and expense. Again, analyzes can help reduce the cost as well as the timeline.

- **Margins:** Knowledge of available margins is needed for a variety of purposes, e.g., to establish a safe operating envelope or to deal quickly with abnormal situations. To determine the margin available in a design solely from tests, one would need to perform a large number of experiments. Again, time and expense for these can be reduced through analyzes.

For these conflicting reasons, some situations are better addressed through tests, whereas others require a judiciously balanced combination of tests and analyzes. Appropriate combinations of tests and analyzes must be tailored to a variety of factors such as (a) features of the specific change in design, (b) completeness and level of knowledge of relevant damage mechanisms, and (c) specific features, capabilities, and capacities of available test facilities and analytical tools. For example, different combinations of tests and analyzes have been used to verify the CANFLEX fuel design [Hastings *et al.*, 1989], the ACR fuel design [Reid *et al.*, 2008], and the 37M fuel design [Daniels *et al.*, 2008]. In the following sections, we describe a fuel design verification process that combines tests and analysis.

To craft an optimal program of comprehensive design analyzes, a sound knowledge is needed of credible damage mechanisms during the conditions for which fuel integrity needs to be ascertained. A few selected damage mechanisms have been described in detail in earlier sections of this chapter. An overview compilation of all currently known credible and significant damage mechanisms is given in the next subsection.

10.1 Damage Mechanisms

Most discussions about fuel damage revolve around two types of damage: primary and secondary. A primary damage mechanism is one that creates the *initial* hole or break in Zircaloy or is an important precursor to it. Secondary damage—usually from zirconium hydrides—is a consequence of primary damage. This section focusses on mechanisms for primary damage. Secondary damage is discussed in Section 12.1.

Based on first principles and confirmed by a comprehensive search of the available literature [Sun *et al.*, 2010], 18 primary damage mechanisms have been identified for CANDU fuel [Tayal *et al.*, 2008-1], of which only three are described in detail in the preceding sections for reasons of space. All eighteen are, however, listed in the following sections. For simplicity in the following discussion, the primary damage mechanisms are classified into three broad groups: thermal damage, structural damage, and compatibility considerations [Tayal *et al.*, 2008-1] and are described below in turn.

10.1.1 Thermal Damage (“T” Series)

Four thermally driven mechanisms can potentially damage the fuel, as described below.

Pellet melting

If the pellet melts, the resulting volumetric expansion of the pellet may potentially push the sheath past its breaking point. Alternatively, molten UO₂ may potentially flow into contact with Zircaloy and melt it by its contained heat.

Zircaloy-UO₂ is another system with a low-melting-point alloy. Hence, strictly speaking, UO₂ does not have to heat the Zircaloy all the way to its melting point to form a liquid alloy.

Melting of Zircaloy or its alloys

Insufficient cooling may potentially melt the Zircaloy, impeding its ability to contain fission products.

The fuel sheath also contains Zircaloy/beryllium eutectic and other alloys in that neighbourhood. Their melting points are lower than that of the parent Zircaloy, and therefore insufficient cooling may potentially melt these alloys. This could detach the pads from the sheaths, destroying their functionality.

Crevice corrosion

Crevice corrosion can potentially occur in crevices such as between bearing pads and the pressure tube or between pads and the sheath. The crevices restrict the flow of coolant. Coolant can boil off in the near-stagnant conditions in the crevice, which in turn can increase the concentration of chemicals such as lithium in the crevice. Lithium, in the form of lithium hydroxide, is added to the coolant to control its pH. The resulting elevated concentration of lithium can potentially accelerate Zircaloy corrosion.

Overheating by contact

If a heated surface such as the sheath contacts a neighbouring surface such as another sheath or the pressure tube, there is potential for reduced local cooling and hence overheating of the fuel, the pressure tube, or both.

10.1.2 Structural Damage (“S” Series)

Structural damage can potentially be caused through nine mechanisms, as described below.

Internal overpressure

In conjunction with a corrosive internal environment and local hydrides, excessive internal pressure in a fuel element can in principle cause cracks at two locations of stress concentration for primary stresses: at the sheath/endcap junction, and at the junction of the sheath and the pad. In practice, to date such cracks have been observed primarily at the sheath/endcap junction.

Environmentally assisted cracking during power ramps

During power ramps, irradiation-embrittled Zircaloy can experience high stresses and strains in the presence of a corrosive internal environment and local hydrides. This combination can potentially crack the sheath at locations of concentration for secondary stresses and strains—at circumferential ridges and at sheath/endcap junctions—through environmentally assisted cracking.

Static mechanical overstrain

During a variety of situations such as refuelling, structural components of the fuel bundle can potentially be exposed to relatively high loads, relatively sparse support, or both, leading to a potential for static mechanical overstrain.

Uncontrolled loss of geometry

This term refers to situations that can potentially lead to buckling, which in turn can lead to uncontrolled loss of geometry.

Fatigue

Alternating stresses caused by vibration (e.g., induced by flow, turbulence, or both), power manoeuvring, and load following can expose the fuel to potential failure through fatigue.

Fuel mechanical rupture due to impact

Situations such as refuelling or starting and restarting of coolant pumps can potentially impose significant impact loads. This is more damaging if it occurs after some amount of irradiation embrittlement of Zircaloy.

Primary hydride failure

A fuel element can pick up hydrogen or deuterium from a variety of sources. The hydrogen and deuterium tend to concentrate at relatively cooler locations and/or at locations of relatively higher stress. Excessive local hydrides and deuterides can reduce the local ductility of Zircaloy, rendering it less capable of carrying its load.

Oxide spalling and hydride lens formation

Some amount of corrosion is unavoidable in Zircaloy at the high temperatures and chemistry of the coolant. If the oxide surface is too thick, it can spall away. This can create local temperature gradients, which can form local hydride/deuteride deposits called “hydride lenses”. Loss of crud from a uniform layer of crud would have a similar effect. A hydride lens embrittles Zircaloy locally, reducing its capacity to carry load.

Insufficient ductility during post-irradiation handling

To enable post-irradiation handling of fuel, it is prudent to limit the amount of hydrides and deuterides in irradiated Zircaloy so that it has reasonable residual ductility to resist its anticipated loads.

10.1.3 Compatibility Considerations (“C” Series)

Five mechanisms can cause potential incompatibilities, as described below.

Interaction loads on the fuel string

This mode of damage refers to the potential expansion of the fuel string to become longer than the available length of the cavity in the fuel channel.

Dimensional incompatibility of a fuel bundle

This mode of damage refers to the possibility of the in-service on-power dimensions of the fuel bundle becoming larger than the available space through processes such as creep and thermal expansion. This can potentially generate unanticipated large stresses that may damage the fuel.

Spacer pad fretting

Excessive fretting of spacer pads due to vibration can potentially rub the corner of a spacer pad into the adjacent sheath, potentially creating a hole in the sheath, or can reduce the gap between elements below the design minimum required for heat removal by the coolant.

Jamming

This mode refers to the possibility that in-service on-power dimensions of the fuel bundle may become such that the fuel bundle cannot pass—easily or at all—through the fuel channel. For example, this can potentially occur due to interlocking of multiple spacers or due to excessive distortion.

Damage to pressure tubes

Bearing pads can cause fretting, sliding wear, and crevice corrosion in pressure tubes.

10.2 Acceptance Criteria and Integration

Acceptance criteria are needed to determine whether or not damage from the above mechanisms is within acceptable limits. Table 4 lists a set of acceptance criteria [Tayal *et al.*, 2008-1].

Table 4 Fuel design acceptance criteria for normal operating conditions

[Source: Tayal *et al.*, 2008-1]

Damage Consideration	Acceptance Criterion
“T Series”: Thermal Integrity	
Fuel element failure due to fuel melting	T1: Local temperature in all parts of the pellet shall stay below the melting point of the pellet, with a minimum acceptable margin.
Fuel element failure due to sheath melting	T2: Local temperature in all parts of the sheath and the endcap shall stay below the local melting point of the material, with a minimum acceptable margin.
Fuel element failure due to crevice corrosion	T3: Underneath a bearing pad or spacer pad, the temperature at the sheath outer surface shall be less than that required to cause crevice corrosion of the sheath, with a minimum acceptable margin.
Fuel or pressure tube failure due to overheating by contact	T4: Fuel bundle dimensional changes (e.g., due to irradiation, loads, creep, bowing, etc.) shall maintain a minimum acceptable clearance between neighbouring sheaths or endcaps and also between the pressure tube and its sheath/encap.
“S Series”: Structural Integrity	
Fuel sheath failure due to	S1: The excess of internal pressure over coolant pressure shall be less than the pressure that causes cracking in the fuel sheath or in

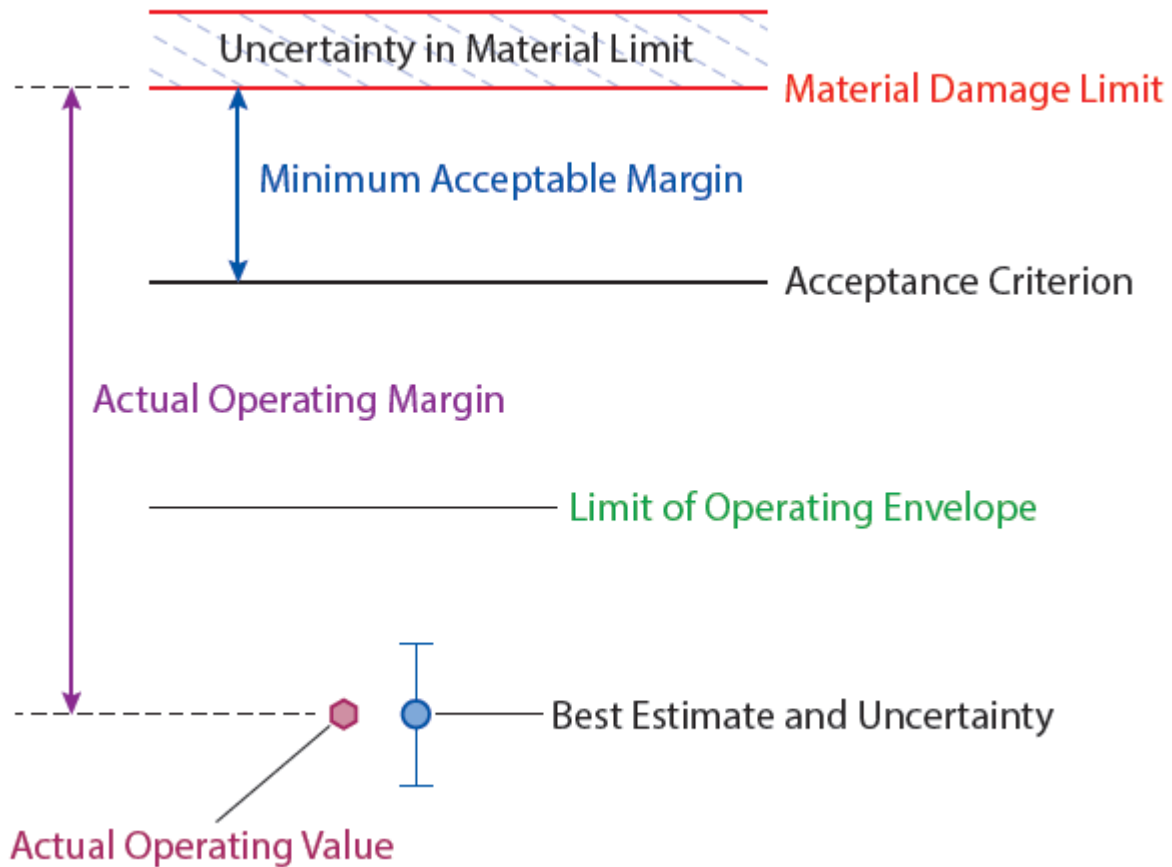
Damage Consideration	Acceptance Criterion
overpressure	the sheath/endcap junction, with a minimum acceptable margin.
Fuel sheath failure due to environmentally assisted cracking due to power ramps	S2: Stresses and strains (or related powers and ramps) during power increases in fuel elements at circumferential ridges and at sheath/endcap junctions shall be less than the appropriate defect thresholds (with a minimum acceptable margin), including the effects of pellet chips, if any.
Fuel failure due to static mechanical overstrain	S3: Local principal strain (elastic plus plastic) shall be less than the available ductility minus the minimum acceptable margin, and local creep strain shall be less than the creep rupture strain, with a minimum acceptable margin.
Fuel failure due to uncontrolled loss of geometry	S4: Axial and related loads on the fuel bundle shall be less than the bundle buckling strength, with a minimum acceptable margin.
Fuel failure due to fatigue	S5: Cumulative fatigue damage from repeated cycles of alternating stresses and strains shall be less than the allowable fatigue life, with minimum acceptable factors of safety on the magnitude of cyclic strain and on the number of cycles.
Fuel mechanical rupture due to impact of loads such as refuelling and/or start/restart	S6: Strain energy density during impact shall be less than that required to crack or break any metallic component of the fuel bundle, with a minimum acceptable margin.
Primary hydride failures	S7: Equivalent concentration of internal hydrogen of an as-fabricated fuel element, from all sources excluding the sheath, shall not exceed the minimum acceptable limit.
Formation of a local hydride lens due to oxide and crud	S8: The combined thickness of oxide and crud on the fuel sheath outer surface shall be less than the amount required for spalling from the surface, with a minimum acceptable margin.
Failure due to insufficient ductility during post-irradiation handling	S9: The volume-average concentration of hydrogen (in the form of soluble atomic hydrogen and equivalent hydrides and deuterides, including their orientation) over the cross section of load-bearing components shall be less than the amount required to retain sufficient ductility, with a minimum acceptable margin.
“C” Series: Compatibility	
Failure due to excessive interaction loads along the	C1: Maximum length of the fuel string (e.g., in the fuel channel) shall be less than the minimum available cavity (e.g., between the

Damage Consideration	Acceptance Criterion
fuel string	shield plug or latches), with a minimum acceptable margin.
Failure from damage by interfacing equipment	C2: Net dimensions, including dimensional changes, throughout fuel bundle residence in the reactor shall be within specified limits for interfacing equipment.
Fuel sheath failure due to fretting of pads	C3: At spacer pads, total wear from all sources such as lateral vibrations, axial vibrations, fretting, sliding, and erosion shall be less than that which brings any part of a spacer in contact with a neighbouring sheath, with a minimum acceptable margin.
Fuel bundle jamming	C4: To enable passage of fuel through the reactor in all fuel handling operations, the axial force required to move the bundle shall be within design allowance, including all pertinent considerations such as on-power deformations, in-service contacts with neighbouring components, and changes in material properties.
Protection of pressure tube from bearing pads	C5: Depth of crevice corrosion, sliding wear, and fretting wear in the pressure tube from fuel bearing pads shall be within specified allowances.

Many complex processes occur in a fuel element. Therefore, in real life, one seldom has complete knowledge of all credible combinations of important variables involving design, manufacturing, and operating conditions that might fail the fuel, nor the luxury of performing an essentially infinite number of experiments that would cover them all. Therefore, in real life, we must deal satisfactorily, not only with what is known, but also with what is not.

In some situations, we know what we don't know—the known unknowns. In other situations, we don't even know what we don't know—the unknown unknowns. "Known unknowns" are usually included in assessments through quantified uncertainties. However, "unknown unknowns" are usually addressed through margins contained within acceptance criteria.

Figure 29 illustrates the concept of margin within an acceptance criterion; the figure labels it as "Minimum Acceptable Margin". Such a margin reflects expert judgment about the "unknown unknowns" in a given technology area. Therefore it can change with time as additional knowledge becomes available and/or as improved technologies for design, production, and/or assessments are developed and incorporated into the product.



[After Sun *et al.*, 2009]

Figure 29 Margins in criteria and analyzes

As noted earlier, a variety of assessment techniques are used to evaluate a product, including engineering judgment, tests, and analyzes. Their combinations are used through a large set of assessments that can potentially be performed as needed to confirm that acceptance criteria have been met. Some illustrative tests for prototype CANDU fuel, shown in Table 3, have already been mentioned.

Most fuel analyzes tend to be highly non-linear and multi-disciplinary. In addition, several analyzes require strong considerations of significant feedbacks among many complex processes. For this reason, the nuclear fuel industry frequently uses a number of computer codes to perform analyzes. An illustrative list is given in Table 5.

Table 5 Illustrative list of computer codes used at AECL for fuel analyzes

Program	Description
ABAQUS	This finite-element code is used for structural analyzes of fuel strings, especially in the presence of non-linearities of intermediate level. Typical examples include: (a) determination of stresses in the fuel string resting on side stops and experiencing hydraulic drag load, and (b) impact stresses during loading of fresh fuel bundles. For an overview and further details of this code, contact Dassault Systèmes, France.
ASSERT	This sub-channel code is used to assess thermal-hydraulic conditions in the fuel channel, including the effects of heat transfer between the fuel and the coolant. Key results include distributions of flow and voids, pressure drop, and critical heat flux. For an overview and further details of this code, contact Atomic Energy of Canada Limited, Canada.
BEAM	This code provides a fast and simple tool to assess several aspects of the mechanical behaviour of a fuel element. Key results include axial and lateral stiffnesses of a fuel element, frequencies of lateral vibrations and resulting elastic stresses, collapse pressure of a sheath, and buckling strength of a fuel element. An overview is available from M. Tayal <i>et al.</i> , "Assessing the Mechanical Performance of a Fuel Bundle: BEAM Code Description", <i>Proceedings, Third International Conference on CANDU Fuel</i> , Canadian Nuclear Society, Pembroke, ON, 1992, October 4-8.
BOW	This finite-element code is used to assess the lateral deformations of fuel elements and bundles, e.g., bow, sag, and droop. An overview is available from M. Tayal, "Modelling the Bending/Bowing of Composite Beams such as Nuclear Fuel: the BOW Code", <i>Nuclear Engineering and Design</i> , vol. 116, pp. 149-159 (1989).
ELESTRES	This finite-element code is used to calculate several thermal, mechanical, and microstructural responses of a fuel element. Key results include sheath and pellet temperatures; fission gas release and internal pressure; and sheath strain as a result of expansion, contraction, and hourglassing of pellets and the sheath. An overview is available from M. Tayal, "Modelling CANDU Fuel under Normal Operating Conditions: ELESTRES Code Description", <i>Report CANDEV-86-110</i> , published by CANDU Owners' Group; also <i>Report AECL-9331</i> , published by Atomic Energy of Canada Limited, February 1987.
FEAST	This finite-element code is used to model detailed local stresses, strains, and deformations such as at circumferential ridges, at sheath/endcap junctions, and in a sheath above an axial gap. An overview is available from M. Tayal, "FEAST: A Two-Dimensional Non-Linear Finite-Element Code for Calculating Stresses", <i>Proceedings, Seventh Annual Conference of the Canadian Nuclear Society</i> , Toronto, Ontario, Canada, June 8–11, 1986.

Program	Description
FEAT	This finite-element code is used to model local temperatures such as the effects of end-flux peaking and local temperatures pertinent to crevice corrosion and braze voids. An overview is available from M. Tayal, "The FEAT Finite-Element Code to Calculate Temperatures in Solids of Arbitrary Shapes", <i>Nuclear Engineering and Design</i> , Vol. 114, pp. 99-114 (1989).
FEED	This finite-element code is used to model diffusion of hydrogen/deuterium in Zircaloy. Key results include concentrations of hydrogen at various locations. An overview is available from L. Lai <i>et al.</i> , "A Method to Model Hydrogen Precipitation", <i>Proceedings, 11th International Conference on CANDU Fuel</i> , Canadian Nuclear Society, Niagara Falls, 2010.
INTEGRITY	This model uses a semi-mechanistic approach to improve calculations of environmentally assisted cracking due to power ramps by accounting for a variety of effects that are not included in the current database of available empirical correlations, such as varying pellet density, sheath diameter, coolant pressure, and coolant temperature. An overview is available from M. Tayal <i>et al.</i> , "INTEGRITY: A Semi-Mechanistic Model for Stress Corrosion Cracking of Fuel", <i>IAEA Technical Committee Meeting on Water Reactor Fuel Element Modelling at High Burnup and its Experimental Support</i> , Windermere, United Kingdom, AECL-10792, September 19–23, 1994.
LONGER	This code calculates conditions related to sheath collapse. Key results include pressure for elastic instability, critical pressure for excessive longitudinal ridges, and pressure for axial collapse. An overview is available from U. K. Paul <i>et al.</i> , "LONGER: A Computer Program for Longitudinal Ridging and Axial Collapse Assessment of CANDU Fuel", <i>Proceedings, 11th International Conference on CANDU Fuel</i> , Canadian Nuclear Society, Niagara Falls, Ontario, 2010.
LS DYNA	This finite-element code overlaps the functionality of ABAQUS code and can also be used for analyzes of strength, impact, and vibration of fuel strings. For an overview and further details of this code, contact Livermore Software Technology Corporation, U.S.A.
NUCIRC	For purposes of fuel analyzes, this thermal-hydraulic code is used to calculate critical channel power. For an overview and further details of this code, contact Atomic Energy of Canada Limited, Canada.

11 Operating Constraints and Inputs to the Safe Operating Envelope

For a specific project application, one would perform assessments (tests and analyzes) as mentioned above to ascertain that the chosen fuel design meets the specified design requirements without failing (i.e., by showing that the fuel acceptance criteria are met). The assessments would at the same time establish the limits, or constraints, on certain plant parameters such that the specified fuel acceptance criteria are met. These plant operating constraints, as

derived from fuel assessments, and similar constraints derived from assessments of all other systems are then used in safety analysis to establish the plant's safe operating envelope.

12 Removal of Fuel Bundles Containing Defects

CANDU reactors have an enviable record of very low fuel defect rates, as noted in Section 2.3. Nevertheless, defects in fuel bundles do occasionally occur. CANDU reactors also have a unique ability to detect, locate, and discharge fuel bundles which contain defective elements without shutting the reactor down. This capability is described in this section. However, we first give a brief summary of how a small primary defect in a fuel element can grow with time into a bigger hole that releases progressively larger amount of radioactivity to the coolant.

Fundamental aspects of such deterioration have been discussed by Lewis *et al.* [1988]. Section 12.1 below is based largely on a document published by the CANDU Owners' Group (COG). Sections 12.2 and 12.3 below are based on an IAEA document [IAEA NF-T-2.1, 2010].

12.1 Deterioration of Primary Defects in Fuel Elements

As noted in Section 10.1 of this Chapter, there are eighteen mechanisms that can cause a failure (primary defect) in CANDU fuel, some in fuel bundles and some in fuel elements. In this section, we consider only one form of defect, albeit the most important, that of a crack or a hole developing in a fuel element, to illustrate how the defective fuel detection and removal system functions in a CANDU reactor. Detection and removal of fuel bundles that have experienced other types of defects would follow a similar procedure, although some fuel bundle defects (such as a bundle becoming stuck in a fuel channel) may require different or additional steps. Please see Section 10.1 for a description of primary defects and how they are caused.

If a crack or hole in the sheath of a fuel element (a primary defect) permits coolant water to penetrate the fuel element, the hole can grow progressively bigger with time through a process called "post-defect deterioration", resulting in release of progressively larger amounts of radioactive fission products into the coolant. This can eventually pose a health hazard to station staff. Therefore, fuel bundles that contain defective fuel elements must be discharged from the reactor before the crack or hole in the fuel element becomes too big.

As explained below, post-defect deterioration of this type of primary defect in fuel elements occurs due to a combination of three main factors:

- secondary hydriding of the sheath (or "deuteriding" when heavy water is used as a coolant, as it is in CANDU; "hydriding" will be used hereafter in this section for simplicity);
- stresses in the sheath; and
- oxidation and swelling of UO_2 .

Secondary Hydriding: Secondary hydriding refers to Zircaloy-hydrogen compounds that are formed in the sheath as a consequence of a primary defect. Water enters the fuel element through the primary crack or hole. At the higher temperature inside the fuel element, the water turns into steam and can better react chemically with Zircaloy and with the UO_2 pellet. The chemical reaction oxidizes some of the Zircaloy and turns some of the UO_2 into higher oxide(s). This chemical reaction also releases hydrogen radicals from steam. Radiolytic decomposition also releases hydrogen radicals from water. The free hydrogen enters the metal matrix of the Zircaloy sheath and migrates by diffusion to areas of higher stress and lower tempera-

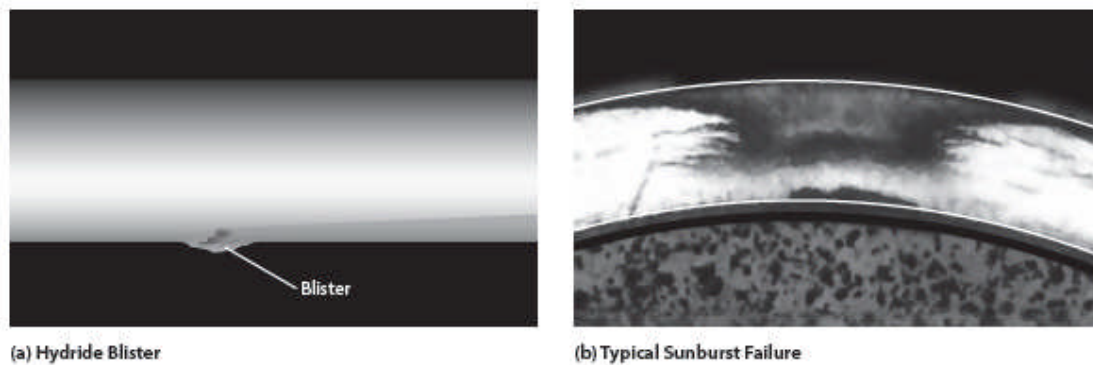
ture. Therefore, the hydrogen often accumulates in localized areas such as at the relatively cooler outer surface of the sheath. When the local concentration of hydrogen exceeds the local solubility limit, the excess hydrogen precipitates as hydrides, which are called secondary hydrides. Once hydrides have formed, they can grow by preferentially absorbing additional hydrogen from within the pellet/sheath gap. High levels of hydrides embrittle Zircaloy, leaving it less able to resist stresses and strains.

A number of pertinent factors may vary along the length of the fuel element, for example the local temperature, the local rate of decomposition, and the local oxidation kinetics of UO_2 and of Zircaloy. For this reason, secondary hydriding generally occurs at some distance away from the primary hole.

Sheath Stresses: The volume of compound hydride is about 16% larger than the volume of the parent Zircaloy. This creates geometric incompatibility among neighbouring materials, which in turn leads to large stresses in the hydride and in the Zircaloy surrounding the hydride. When these stresses become high enough, they can cause cracks in the layer of zirconium oxide which exists on the inside surface of the sheath. This in turn enables additional hydrogen to enter the sheath. Moreover, the hydrides can produce cracks that pass—either fully or partly—through the sheath wall. All cracks enable further ingress of hydrogen; through-wall cracks also enable more water to enter the fuel element.

Oxidation and Swelling of UO_2 : Reaction of water and UO_2 results in higher concentrations of uranium oxides, commonly labelled $\text{UO}_{(2+x)}$. The higher oxides have lower density, and therefore lower thermal conductivity and higher nominal volume, than UO_2 . The lower thermal conductivity increases the temperature and hence the thermal expansion of the pellet, which combines with the higher nominal volume to swell the pellet. The expanding pellet then increases the width of the crack in the Zircaloy sheath.

These processes can lead to a hole, often caused by a loss of material from the outside surface of the sheath, called a “blister”. Figure 30(a) provides an illustrative example. Holes due to secondary damage are often much bigger than holes from primary damage and hence can release significant radioactivity, and even some UO_2 , into the coolant. For this reason, it is prudent to discharge a fuel bundle that contains a failed fuel element before significant secondary damage to the sheath occurs. Fortunately, the process of forming secondary defects often takes some time, and CANDU reactors are unique in being able to: (1) detect fuel element defects that release radioactive fission products into the coolant, (2) identify the fuel channels that contain bundles with defective fuel elements, (3) discharge these bundles before the defects in the fuel-element sheath become too big, and (4) do all this without shutting the reactor down. The next section summarizes the techniques to do this.



[Courtesy: COG]

[Source: IAEA, 2010]

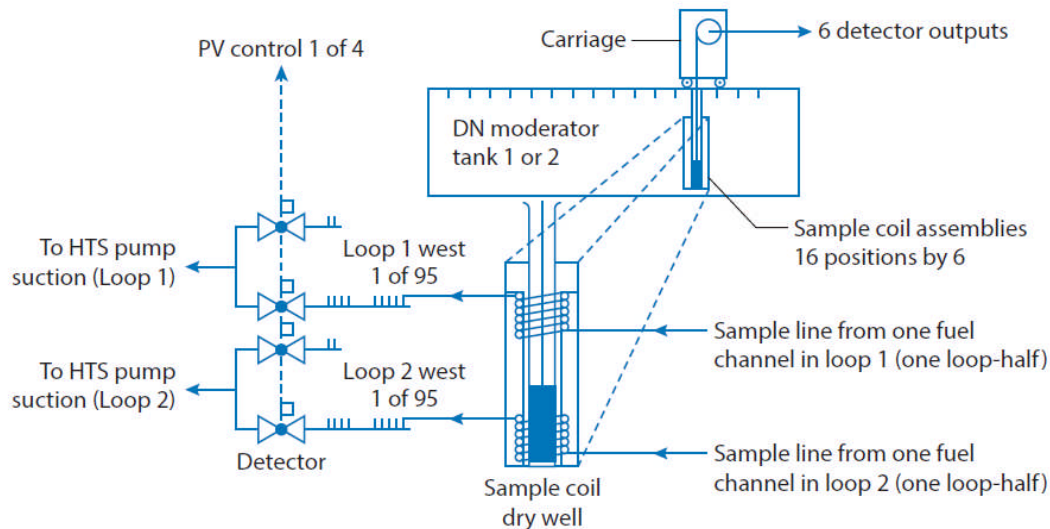
Figure 30 Secondary hydriding

12.2 Defect Removal Systems

Three systems have been developed to detect and locate defective fuel elements that release radioactive fission products into the coolant: (1) gaseous fission product (GFP), (2) delayed neutron (DN), and (3) feeder scanning (FS) systems.

The GFP system monitors continuously when the reactor is at power and detects a general increase of radioactivity in the coolant when a defect occurs in a fuel element anywhere in the core. This system alerts the operator that a defect has occurred and identifies the coolant loop in which the defect is located, thereby eliminating 50% of fuel channels from the “suspects” list.

The DN system is also used when the reactor is at power, but does not monitor continuously. The activity-sensing portion of the DN system is put into operation after a defect signal is indicated by the GFP system. The DN system is used to identify the fuel channel that contains the defective elements by detecting activity in the coolant at the downstream end of a fuel channel [Manzer *et al.*, 1984]. In a closed-loop configuration, sampling lines attached to outlet feeders continuously carry small streams of coolant to a common room within the reactor building (see Figure 31) and return the streams back into the coolant circuit downstream of the outlet header. In the sampling room, BF3 sensors detect delayed neutrons emitted by short-lived fission-products (^{137}I and ^{87}Br). The lengths of the sampling lines (custom-sized for each channel) are such that the delivery of the sample to the sensor takes advantage of the decay half-life of the delayed-neutron precursors. If neutron activity in a coolant sampling line is higher than normal, the corresponding fuel channel is suspected of containing a fuel bundle with a defective element. The DN system has sufficient sensitivity to locate fuel element defects with very small holes. Bruce and CANDU-6 reactors use the DN system.



[Source: IAEA, 2010]

Figure 31 Schematic diagram of a delayed neutron monitoring system in a CANDU-6 reactor

The FS system is used when a reactor is shut down. It locates the fuel channel that contains the defective element by scanning for activity on the inside surfaces of the outlet feeders connecting the fuel channels to a common outlet header [Lipsett *et al.*, 1976]. The presence of gamma-emitting fission products inside the channel is detected by Geiger-Muller detectors moving within guide tubes that traverse the outlet feeders. If gamma activity in a specific feeder is higher than normal, then the corresponding fuel channel is suspected of containing a fuel bundle that has a (severely) defective element. The FS system locates only defects that have deteriorated to the point of releasing uranium and fission products which deposit immediately downstream of the defect. The Darlington reactors use the FS system.

12.3 Confirmation of Defect Removal

After the channel which has been identified as containing the defect has been refueled in a CANDU reactor, the defective fuel element is confirmed to have been discharged by various methods, again depending on the station:

- Inspecting the discharged bundles in the bay;
- Monitoring gamma activity near the spent fuel handling system when bundles are en route from the reactor to the fuel bay (wet or dry sipping) and/or when they are residing in the fuel bay (wet sipping);
- Monitoring delayed neutron activity of the coolant at the outlet end of the channel during refuelling.

The first method provides direct confirmation that a bundle that contains a defective fuel element has been removed. Portable underwater TV cameras are used at multi-unit stations operated by Ontario Power Generation, whereas periscopes are used at single-unit CANDU-6 stations [Lipsett, 1976]. Photographs of the defective elements confirm that a defective bundle has been removed.

The second and third methods provide indirect confirmation that a bundle containing a defective element has been removed by monitoring gamma activity near the spent fuel handling system or in fuel bays. At Bruce, dry sipping techniques [MacDonald *et al.*, 1990] are used to monitor airborne gamma activity in the air chamber that separates the heavy water side of the spent fuel transfer mechanisms from the light water environment of the fuel bay. A higher-than-normal signal that lingers after bundles have been transferred usually indicates the presence of a defective element.

Two other techniques have also been developed at CANDU-6 stations to confirm that fuel bundles containing defective elements have been discharged from the core. One technique depends on the radiation levels of fission products in the heavy water inside the fuelling machine. Before discharge of irradiated fuel bundles to a bay, heavy water from the fuelling machine is transferred to a nearby drain tank. The presence of a defect is indicated when gamma fields near the tank trigger an alarm that monitors gamma in the area. Another technique developed in the inspection bay at Point Lepreau is based on “wet sipping”, or measuring the gamma activity of water samples near recently discharged bundles. Again, a defect is confirmed if gamma activity is unusually high.

Monitoring delayed neutron activity at the outlet end of a fuel channel during refuelling also provides some confirmation that a fuel bundle containing a defective element is being discharged from the core [Manzer, 1985]. At CANDU-6 sites, special refuelling procedures are sometimes used which involve allowing the fuel bundles inside the channel to move slowly with the flow while monitoring the DN signal of the channel. When the signal drops to below “pre-defect” levels, this indicates that the fuel bundle containing the defect has been pushed outside the core boundary.

13 Closure

To restate a point made in Section 2.3, the defect rate is remarkably low in CANDU fuel—almost in the range of impurities found in most substances. An IAEA survey has reported the following world-wide fuel defect rates between 1994 and 2006 [IAEA, 2010]:

- 94 failed rods per million discharged (ppm) in WWERs;
- 87 ppm in PWRs;
- 65 ppm in BWRs; and
- 3.5 ppm in Canada.

These figures affirm the basic soundness of practices built into all major aspects of CANDU fuel—from research to development, design, fabrication, and operation and the feedbacks among them.

14 Problems

Section 2

Q2.1 – Why is a CANDU fuel “element” able to produce 30 times more heat than an electric element of a similar size?

Q2.2 – List at least six conditions that occur during at-power operation of CANDU fuel that challenge the integrity of the fuel.

Q2.3 – Name the components of a typical CANDU fuel bundle.

Q2.4 – Why is the uranium that is used in CANDU fuel bundles in the form of uranium dioxide, rather than uranium metal, for instance?

Q2.5 – Why is helium used to purge the air out of fuel elements during fabrication?

Q2.6 – For a fixed bundle power, the only means that the fuel designer has at his disposal to change the individual element rating is to use more or fewer elements. Using more elements (subdivision) permits the coolant to be nearer the source of the heat at more locations, leading to lower UO_2 temperature and reduced threats from many thermally driven damage mechanisms. What are some of the negative effects of subdivision?

Q2.7 – Experience and fundamental engineering considerations have shown that CANDU fuel bundles can experience 18 different modes of failure in a reactor. Name the three general groups into which the modes are grouped and provide the principal characteristic of each group.

Section 3

Q3.1 – What does “burnup” measure, and what units is it expressed in?

Q3.2 – A CANDU fuel element contains UO_2 pellets 20 mm in diameter and having a density of 10.5 g/cm^3 . At 60 kW/m , how long does it need to accumulate a burnup of 40 MWh/kgU ? Why does this need so much longer than the fuel element of Section 3?

Section 4

Q4.1 – A fuel element has the following characteristics: diameter = 15 mm; sheath thickness = 0.5 mm; Young’s modulus = 80 GPa; Poisson’s ratio = 0.37. Is it elastically stable at 6 MPa? At 7 MPa? At 8 MPa?

Section 6

Q6.1 – What is fission gas?

Q6.2 – Why is it important to maintain fission gas pressure as low as possible?

Q6.3 – Describe the processes involved in the generation, accumulation and release of fission gas into “open” spaces inside the fuel sheath.

Q6.4 – What design features does the fuel designer have at his disposal to control or minimize fuel element internal gas pressure?

Q6.5 – Using the equations presented in Section 6.5, determine the effect of storing the fission gas at pellet centreline temperature compared to that of the pellet interface with the sheath.

What do we learn?

Q6.6 – A fuel element’s free space is 3 ml, and it contains 15 ml of gas at STP. Assuming that all the gas is stored at a uniform temperature of 1400 K, what is the internal pressure of the fuel element? [Hint: Use Equation 5].

Section 7

Q7.1 – Describe three defect types in CANDU fuel that may be caused by excessive stress.

Q7.2 – Describe in qualitative terms the reasons that cracks develop in uranium dioxide pellets at operating conditions.

Q7.3 – A temperature profile is parabolic in a pellet of radius 6 mm. Is the hoop stress tensile or compressive at: 1 cm? 2 cm? 3 cm? 4 cm? 5 cm?

Section 8

Q8.1 – Describe qualitatively the conditions that might lead to environmentally assisted cracking.

Q8.2 – Provide examples of EAC defects that have been observed in CANDU fuel elements.

Q8.3 – Recognizing the three different effects that can cause EAC defects in CANDU fuel elements, provide a qualitative description of reactor operation that could lead to EAC defects.

Q8.4 – What parameters from operating reactors have been correlated to provide an indication of potential fuel failure due to EAC? Draw a figure to show the relationship.

Q8.5 – Describe the mitigating parameters that have been adopted by CANDU designers and operators to minimize EAC defects.

Q8.6 – A non-CANLUB fuel bundle experiences a power ramp from 25 kW/m to 50 kW/m at 140 MWh/kgU. What is its probability of having a defect? What would the defect probability be if it were CANLUB fuel?

Section 9

Q9.1 – Describe the coolant conditions that may lead to fuel vibration.

Q9.2 – Describe the type of damage that fuel can experience as a result of vibration.

Q9.3 – A C6 fuel element has the same dimensions as in the illustrative example of Section 9.1.6, with the exception that its assembly weld has inadvertently been manufactured with a diameter of 3 mm. Coincidentally, it is also destined to be loaded into a channel where the amplitude of lateral vibration is expected to be 30 micrometers. What nominal stresses are expected in the endplate and in the assembly weld? Are fatigue failures likely by this mechanism?

Section 10

Q10.1 – How many damage mechanisms have been shown to affect CANDU fuel?

Q10.2 – How many thermal damage mechanisms (“T” series) are there? Provide a brief description of each.

Q10.3 – How many structural damage mechanisms (“S” series) are there? Provide a brief description of each.

Q10.4 – How many compatibility damage mechanisms (“C” series) are there? Provide a brief description of each.

Q10.5 – List the design acceptance criteria for CANDU fuel.

Q10.6 – With the aid of a diagram, show the relationship of acceptance criteria to other relevant parameters, e.g., the material damage limit.

Q10.7 – What is the purpose of assigning margins in relation to acceptance criteria?

Q10.8 – List the qualification tests and assessments used to qualify CANDU fuel bundles.

Section 11

Q11.1 – Name at least one plant operating constraint that is related to ensuring fuel integrity. Are there others?

Q11.2 – How are plant operating constraints defined by system designers such as fuel designers used to ensure safe plant operation?

Section 12

Q12.1 – What is the most common defect type that occurs in CANDU fuel during plant operation?

Q12.2 – What are the principal characteristics of the most common defect type that makes its detection possible while the plant is in operation?

Q12.3 – What is secondary hydriding? Explain the mechanism and how it affects the integrity of the fuel element.

Q12.4 – Explain why it is important to remove a defective fuel element from an operating reactor as soon as the defect is detected.

Q12.5 – Name the three systems used in CANDU reactors to assist in the detection and removal of defective fuel while the reactor is at power and explain briefly how each is used.

Q12.6 – Name three techniques used to confirm that a bundle containing a defective fuel element has been discharged from the channel and explain briefly how each works.

15 References

- A. H. Booth, "A Method of Calculating Fission Gas Diffusion from UO_2 Fuel and its Application to the X-2-f Loop Test", Atomic Energy of Canada Limited, *Report AECL-496* (1957).
- G. H. Bryan, "Application of the Energy Test to the Collapse of a Long Thin Pipe under External Pressure", *Proceedings of Cambridge Phil. Society*, Vol. 6, p. 287 (1888).
- R. M. Carroll and O. Sisman, "In-Pile Fission Gas Release from Single-Crystal UO_2 ", *Nuclear Science and Engineering*, vol. 21, pp. 147–158 (1965).
- T. Daniels, H. Hughes, P. Ancker, M. O'Neil, W. Liao, and Y. Parlatan, "Testing and Implementation Program for the Modified Darlington 37-Element Fuel Bundle", *Proceedings, 10th International Conference on CANDU Fuel*, Canadian Nuclear Society (2008).
- A. Fick, "Über Diffusion", *Phil. Mag.*, vol. 10, pp. 59–86 (1855).
- M. R. Floyd, D. A. Leach, R. E. Moeller, R. R. Elder, R. J. Chenier, and D. O'Brien, "Behaviour of Bruce NGS-A Fuel Irradiated to a Burnup of ~ 500 MWh/kgU", *Proceedings, Third International Conference on CANDU Fuel*, Chalk River, Canadian Nuclear Society, pp. 2-44 to 2-60 (1992).
- M. Gacesa, V. C. Orpen, and I. E. Oldaker, "CANDU Fuel Design: Current Concepts", *IAEA/CNEA International Seminar on Heavy Water Fuel Technology*, San Carlos de Bariloche, Argentina, 1983. Also *Report AECL-MISC 250-1 (Rev. 1)*, published by Atomic Energy of Canada Limited, 1983.
- J. Gere and S. P. Timoshenko, *Mechanics of Materials*, PWS, Fourth Edition (1997).
- I. J. Hastings, "Structures in Irradiated UO_2 Fuel from Canadian Reactors", Atomic Energy of Canada Limited, *Report AECL-Misc-249* (1982).
- I. J. Hastings, A. D. Lane, and P. G. Boczar, "CANFLEX: An Advanced Fuel Bundle for CANDU", *International Conference on Availability Improvements in Nuclear Power Plants*, Madrid, Spain. Also *Report AECL-9929*, published by Atomic Energy of Canada Limited (1989).
- IAEA, "Review of Fuel Failures in Water-Cooled Reactors", International Atomic Energy Agency, Vienna, *Report NF-T-2.1* (2010).
- J. H. K. Lau, M. Tayal, E. Nadeau, M. J. Pettigrew, I. E. Oldaker, W. Teper, B. Wong, and F. Iglesias, "Darlington N12 Investigation: Modelling of Fuel Bundle Movement in Channel under Pressure Pulsing Conditions", *Proceedings, 13th Annual Conference*, Canadian Nuclear Society (1992).
- B. J. Lewis, "Fundamental Aspects of Defective Nuclear Fuel Behaviour and Fission Product Release", *Journal of Nuclear Materials*, Vol. 160, pp. 201–217 (1988).
- J. J. Lipsett and W. B. Stewart, "Failed Fuel Location in CANDU-PHW Reactors using a Feeder Scanning Technique", *IEEE Transactions on Nuclear Science*, Vol. NS-23, No. 1, pp. 321-324 (1976).
- R. D. MacDonald, M. R. Floyd, B. J. Lewis, A. M. Manzer, and P. T. Truant, "Detecting, Locating, and Identifying Failed Fuel in Canadian Power Reactors", *Report AECL-9714*, published by Atomic Energy of Canada Limited, Canada (1990).

- A. M. Manzer and R. W. Sancton, "Detection of Defective Fuel in an Operating CANDU-600 MW(e) Reactor", *Proceedings, Conference on Fission Product Behaviour and Source Term Research*, Snowbird, American Nuclear Society, LaGrange Park, Illinois (1984).
- M. J. F. Notley and I. J. Hastings, "A Microstructure-Dependent Model for Fission Product Gas Release and Swelling in UO₂ Fuel", *IAEA Specialists' Meeting on Fuel Element Performance Computer Modelling*, Blackpool, UK, 1978. Also *Report AECL-5838*, published by Atomic Energy of Canada Limited, 1979.
- W. J. O'Donnell and C. M. Purdy, "The Fatigue Strength of Members Containing Cracks", *Proceedings of ASME Petroleum Division*, ASME Paper 63-PET-1 (1963).
- W. J. O'Donnell and B. F. Langer, "Fatigue Design Basis for Zircaloy Components", *Nuclear Science and Engineering*, Vol. 20, pp. 1–12 (1964).
- D. E. Olander, "Fundamental Aspects of Nuclear Reactor Fuel Elements", Energy Research and Development Administration, U.S.A., *Report TID-26711-P1* (1976).
- R. D. Page, "Canadian Power Reactor Fuel", Atomic Energy of Canada Limited, *Report AECL-5609* (1976).
- W. J. Penn, R. K. Lo, and J. C. Wood, "CANDU Fuel—Power Ramp Performance Criteria", *Nuclear Technology*, Vol. 34, pp. 249–268 (1977).
- R. E. Peterson, "Application of Stress Concentration Factors in Design", *Proceedings of the Society for Experimental Stress Analysis*, Vol. 1, pp. 118–127 (1943).
- M. J. Pettigrew, "The Vibration Behaviour of Nuclear Fuel under Reactor Conditions", *Nuclear Science and Engineering*, Vol. 114, pp. 179–189 (1993).
- P. Reid, M. Gacesa, and M. Tayal, "The ACR-1000 Fuel Bundle Design", *Proceedings, 10th International Conference on CANDU Fuel*, Canadian Nuclear Society (2008).
- A. D. Smith, I. J. Hastings, P. J. Fehrenbach, P. A. Morel, and R. D. Sage, "Dimensional Changes in Operating UO₂ Fuel Elements: Effect of Pellet Density, Burnup, and Ramp Rate", Atomic Energy of Canada Limited, *Report AECL-8605* (1985).
- A. Sun and M. Tayal, "Technical Basis for ACR-1000 Fuel Acceptance Criteria", *Proceedings, 11th International Conference on CANDU Fuel*, Canadian Nuclear Society (2010).
- M. Tayal and C. K. Choo, "Fatigue Analysis of CANDU Nuclear Fuel Subjected to Flow-Induced Vibrations", Paper AIAA-84-0959-CP, *25th Structures, Structural Dynamics and Materials Conference*, American Society of Mechanical Engineers, Palm Springs, California, 1984. Also *Report AECL-8331*, published by Atomic Energy of Canada Limited (1984).
- M. Tayal, "Modelling CANDU Fuel under Normal Operating Conditions: ELESTRES Code Description", Atomic Energy of Canada Limited, *Report AECL-9331* (1987).
- M. Tayal, L. M. MacDonald, E. Kohn, and W. P. Dovigo, "A Model for the Transient Release of Fission Products from UO₂ Fuel: GASOUT Code Description", *Nuclear Technology*, Vol. 85, pp. 300–313. Also *Report AECL-9794*, published by Atomic Energy of Canada Limited (1989).
- M. Tayal and G. Chassie, "Extrapolating Power-Ramp Performance Criteria for Current and Advanced CANDU Fuels", *Proceedings, 21st Annual Conference*, Canadian Nuclear Society

(2000).

- M. Tayal, P. Reid, M. Gacesa, A. Sun, E. Suk, and D. Gossain, "ACR-1000 Fuel Acceptance Criteria for Normal Operation and for Anticipated Operational Occurrences", *Proceedings, Tenth International Conference on CANDU Fuel*, Canadian Nuclear Society, Ottawa, Canada (2008-1).
- M. Tayal, A. Sun, M. Gacesa, P. Reid, P. Fehrenbach, B. Surette, and E. Suk, "Mechanism for Power Ramp Failures in CANDU Fuel", *Proceedings, 10th International Conference on CANDU Fuel*, Canadian Nuclear Society (2008-2).
- S. P. Timoshenko, *Strength of Materials, Part 2*, McGraw-Hill, Second Edition (1961).
- S. P. Timoshenko and J. N. Goodier, *Theory of Elasticity*, McGraw Hill, Third Edition (1970).
- J. C. Wood, D. G. Hardy, and A. S. Bain, "Power Ramping Fuel Performance and Development", Atomic Energy of Canada Limited, *Report AECL-6676* (1979).

16 Further Reading

Design Verification

- P. G. Boczar, "CANDU Fuel Design Process", *Ninth International Conference on CANDU Fuel*, Belleville, Canada, Canadian Nuclear Society, 2005.
- J. Chang, S. Abbas, A. Banwatt, M. DiCiano, M. Gacesa, A. Gill, D. Gossain, J. Hood, F. Iglesias, L. Lai, T. Laurie, Y. Ornatsky, U. K. Paul, A. Sun, M. Tayal, S. G. Xu, J. Xu, and P. Reid, "Proof of Design Adequacy for the ACR-1000 Fuel Bundle", *10th International Conference on CANDU Fuel*, Ottawa, Canada, October 5-8, 2008.

History (Early)

- J. A. L. Robertson, "Fuel for Thought", *Nuclear Journal of Canada*, Vol. 1, Issue 4; pp 332-341. Also published in *Proceedings of the Engineering Centennial Conference*, Montreal, 18-22 May, 1987.

Irradiation Tests and Performance

- F. R. Campbell, L. R. Borque, R. Deshaises, H. E. Sills, and M. J. F. Notley, "In-Reactor Measurements of Fuel-to-Sheath Heat Transfer Coefficients Between UO₂ and Stainless Steel", Atomic Energy of Canada Limited, *Report AECL-5400*, 1977.
- T. J. Carter, "Experimental Investigation of Various Pellet Geometries to Reduce Strains in Zirconium Alloy Cladding", *Nuclear Technology*, Vol. 45, No. 2, September 1979, pp. 166-176.
- M. R. Floyd, J. Novak, and P. T. Truant, "Fission-Gas Release in Fuel Performing to Extended Burnups in Ontario Hydro Nuclear Generating Stations", *IAEA Technical Committee Meeting on Fission Gas Release and Fuel Rod Chemistry Related to Extended Burnup*, Pembroke, Canada. Also Atomic Energy of Canada Limited, *Report AECL-10636* (1992).
- M. R. Floyd, Z. He, E. Kohn, and J. Montin, "Performance of Two CANDU-6 Fuel Bundles Containing Elements with Pellet-Density and Clearance Variables", *6th International Conference on CANDU Fuel*, Niagara Falls, Canada. Also Atomic Energy of Canada Limited, *Report AECL-12033*, 1999.

- M. R. Floyd, "Extended-Burnup CANDU Fuel Performance", *International Conference on CANDU Fuel*, CNS, Kingston. Also Atomic Energy of Canada Limited, Report AECL-CONF-01135, 2001.
- D. G. Hardy, A. S. Bain, and R. R. Meadowcroft, "Performance of CANDU Development Fuel in the NRU Reactor Loops", *ANS Topical Meeting on Water Reactor Fuel Performance*, St. Charles, Illinois, pp. 198-206, 1977.
- M. J. F. Notley, A. S. Bain, and J. A. L. Robertson, "The Longitudinal and Diametral Expansion of UO₂ Fuel Elements", AECL-2143, 1964.

Manufacturing and Quality Assurance

- C. Ganguly and R. N. Jayaraj (editors), *Characterization and Quality Control of Nuclear Fuels*, Allied Publishers, 2004.
- M. Gacesa, G. R. Quarrington, W. R. Tarasuk, I. R. Carrick, J. Pawliw, G. McGregor, H. R. Debnam, and L. Proos, "CANDU Fuel Quality and How it is Achieved", Atomic Energy of Canada Limited, Report AECL-7061, 1980.
- R. Sejnoha, "Quality Assurance in CANDU Fuel Design, Development, and Manufacturing", IAEA/INSTN, Saclay (France), October 1992.

Material Science

- R. Adamson, B. Cox, J. Davies, F. Garzarolli, P. Rudling, and S. Vaidyanathan, "Pellet-Cladding Interaction", IZNA-6 Special Topical Report, ANT International, 2006.
- D. L. Hagrman, G. A. Reyman, and R. E. Mason (editors), "MATPRO-Version 11 (Revision 2): A Handbook of Material Properties for Use in the Analysis of Light Water Reactor Fuel Rod Behaviour", EG&G Idaho, Inc., Report NUREG/CR-0479, TREE-1280, Rev.2, 1981.
- A. Sawatzky and C. E. Ells, "Understanding Hydrogen in Zirconium", *Zirconium in the Nuclear Industry: Twelfth International Symposium*, ASTM STP 1354, 2000, pp 32-48.

Modelling and Computer Codes

- J. A. L. Robertson, A. M. Ross, M. J. F. Notley, and J. R. MacEwan, "Temperature Distribution In UO₂ Fuel Elements", *Journal of Nuclear Materials*, pp. 225-262, December 1961. Also AECL-1679.
- M. Tayal, D. Lim, "Recent Uses of the Finite Element Method in Design/Analysis of CANDU Fuel", *Sixth Annual Conference of the Canadian Nuclear Society*, Ottawa. Also Atomic Energy of Canada Limited, Report AECL-8754, 1985.

17 Relationships with Other Chapters

Chapter 8 provides an overview of fuel bundle configuration. Chapters 3 to 5 explain neutron physics that generates heat in the fuel. Chapters 6 and 7 explain how that heat is removed from the fuel bundle and illustrate the internal temperature distribution within a fuel rod. Chapters 14 and 15 explain chemical and metallurgical aspects that relate to corrosion of the fuel sheath. Chapter 13 explains the performance of fuel during postulated accidents. Chapter 18 discusses advanced fuels and fuel cycles; it also summarizes fuel manufacturing. Finally, Chapter 19

describes interim storage and disposal of used fuel.

18 Acknowledgements

The following reviewers are gratefully acknowledged for their hard work and excellent comments during the development of this chapter; their feedback has much improved it.

Peter Boczar
Lawrence Dickson
Rosaura Ham-Su
Paul Chan
Kwok Tsang

Of course the responsibility for any errors or omissions lies entirely with the authors.

Thanks are also extended to Media Production Services, McMaster University, for producing the figures, and to Diana Bouchard for expertly editing and assembling the final copy.